Thermodynamic balancing of a fixed-size two-stage humidification dehumidification desalination system

Karim M. Chehayeb[a], G. Prakash Narayan[b], Syed M. Zubair[c], John H. Lienhard V[a,*]

[a] *Department of Mechanical Engineering, Massachusetts Institute of Technology, Cambridge, MA 02139, USA.*
[b] *Gradiant Corporation, Woburn, MA 01801, USA*
[c] *Department of Mechanical Engineering, King Fahd University of Petroleum and Minerals, Dhahran, Saudi Arabia.*

Abstract

Humidification dehumidification (HDH) is a desalination technology that has shown promise in small scale, decentralized applications. Previous studies on the multi-staging of HDH have used fixed-effectiveness models which do not explicitly account for transport processes in the components. However, to fully understand the effect of the variation of the mass flow rate ratio, it is necessary to implement heat and mass transfer models of the HDH system. In this paper, we model an HDH system consisting of a packed-bed humidifier and a multi-tray bubble column dehumidifier. We study the effect of the mass flow rate ratio on the performance of a fixed-size system, and we consider its effect on the entropy generation and the driving forces for heat and mass transfer. In addition, we define a generalized energy effectiveness for heat and mass exchangers. We also implement an air extraction/injection and simulate a wide range of operating conditions. We define criteria for the best system performance, and we study the effect of the distribution of available area between separate stages. We also present a thorough explanation of why the direction of extraction should always be from the humidifier to the dehumidifier.

Keywords: entropy generation minimization, mass extraction/injection, heat and mass exchanger, bubble column, energy effectiveness, enthalpy pinch

K.M. Chehayeb, G.P. Narayan, S.M. Zubair, and J.H. Lienhard V, "Thermodynamic balancing of a fixed-size two-stage humidification dehumidification desalination system," Desalination, 369:125-139, 3 August 2015.

*Corresponding author
Email address: lienhard@mit.edu (John H. Lienhard V)

Nomenclature

Acronyms

GOR	Gained Output Ratio
HCR	control volume based modified heat capacity rate ratio for HME devices
HDH	Humidification Dehumidification
HE	Heat Exchanger
MR	Water-to-air mass flow rate ratio
RR	Recovery Ratio

Symbols

a	surface area per unit volume of packing [m^2/m^3]
c_p	specific heat capacity at constant pressure [J/kg·K]
D	diameter [m]
g	gravitational acceleration [m/s^2]
$\dot{H}$	total enthalpy rate [W]
H	humidifier height [m]
h	specific enthalpy [J/kg]
h^*	specific enthalpy [J/kg dry air]
h_{fg}	specific enthalpy of vaporization [J/kg]
h_{t}	heat transfer coefficient [W/m^2-K]
K	mass transfer coefficient [kg/m^2-s]
k	thermal conductivity [W/m-K]
$\mathrm{Le_f}$	Lewis factor [-]
$\dot{m}$	mass flow rate [kg/s]
Me	Merkel number, also KaV/L [-]
N_{t}	number of trays in the dehumidifier [-]
Nu_D	Nusselt number based on the diameter [-]
P	absolute pressure [Pa]
Pr	Prandtl number [-]
R	thermal resistance [K/W]
Re	Reynolds number [-]
$\dot{Q}$	heat transfer rate [W]
$\dot{Q}_{\mathrm{in}}$	heat input in the heater [W]
S	Salinity [ppt]
T	temperature [°C]
V	packing volume [m^3]
V_{g}	gas superficial velocity [m/s]

Greek

Δ	difference or change
ε	energy based effectiveness [-]
μ	dynamic viscosity [Pa s]
Ψ	enthalpy pinch [kJ/kg dry air]

ρ	density [kg/m^3]
ω	absolute humidity [kg water vapor per kg dry air]

Subscripts

1	colder stage
2	hotter stage
a	moist air
c	cold stream
col	column
cond	condensate
d	dehumidifier
da	dry air
deh	dehumidifier
f	liquid water
h	humidifier or hot stream
hum	humidifier
HE	heat exchanger
in	entering or inner
lm	logarithmic mean
loc	local quantity
max	maximum
out	leaving
pw	pure water
sa	saturation at air temperature
ss	supersaturation
sw	saturation at water temperature
v	water vapor
w	saline water

1. Introduction

Humidification dehumidification (HDH) is a desalination technology that has received wide attention in recent years. Although it does not compete with existing technologies for desalinating seawater in medium and large scale applications, HDH can be advantageous in decentralized, off-grid desalination applications where fresh water demand ranges up to several thousand cubic meters per day [1, 2]. In addition, the technology does not use membranes and does not include hot metal surfaces, which allows it to treat highly saline water with some oil content without requiring expensive corrosion resistant metals. HDH has recently been commercialized and has succeeded in treating produced water from hydraulically fractured oil and gas wells [3].

A typical HDH system consists of a humidifier, a dehumidifier, and a heater. In this paper we model a water-heated, closed-air, open-water HDH cycle. As shown in Fig. 1, cold air enters the humidifier where it is exposed to hot saline water, which increases its temperature and water content. The hot moist air then enters the dehumidifier where it loses heat to a feed stream of cold saline water flowing through a coil. Water vapor condenses in the dehumidifier and exits the system as a stream of fresh liquid water. The more we preheat the saline water in the dehumidifier the less heat we have to supply in the heater. Improving the energy efficiency of an HDH system is therefore a question of reusing the heat of condensation to heat the feed stream to the highest possible temperature before sending it to the heater.

1.1. Bubble column dehumidifiers in HDH

A major issue that made early HDH systems difficult to commercialize was their need for very large dehumidifiers [4, 5] (up to 30 m^2 for a 1 m^3/day system [6]), which increased their cost of water production greatly. Dehumidifiers contain a very large concentration of air, a noncondensable gas, which leads to very

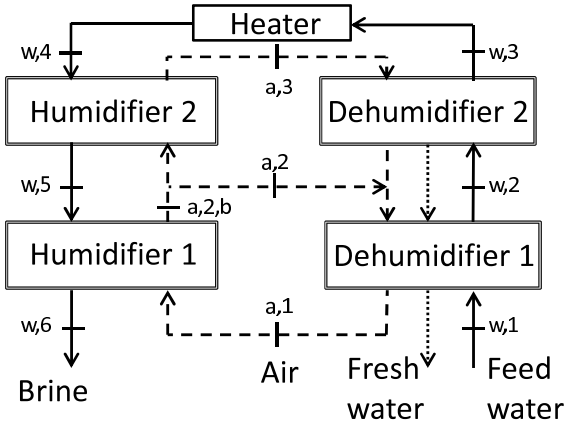

Fig. 1: Schematic diagram representing a water-heated, closed-air, open-water HDH system with a single extraction.

low mass transfer coefficients and increases the surface area needed in conventional dehumidifiers. As a solution to this issue, Narayan et al. [7] suggested the use of short bubble column dehumidifiers in HDH. They measured heat transfer rates that were an order of magnitude higher than those operating in the film condensation regime.

A bubble column is a heat and mass exchanger which, in the case of HDH, serves to transfer heat from a hot moist air stream to a saline feed water stream. Saline water is circulated through a curved coil that is submerged in a column of fresh water, and hot moist air is bubbled from the bottom of the column through a sparger. The air is cooled and dehumidified by transferring heat and mass to the column of fresh water, which in turn transfers the heat to the saline water inside the coil.

Recent studies by Tow and Lienhard [8–10] resulted in an accurate model of bubble columns that was experimentally validated. The model is used in this study, and is discussed in greater detail in Section 2.1. Tow and Lienhard [11, 12] also measured heat transfer rates up to more than 8,000 W/m^2-K in shallow bubble columns, further justifying their use in the dehumidification side of an HDH system.

Although the air and saline water circulate in opposite directions, the bubble column is still effectively a parallel flow configuration: both streams exchange heat with the same pool of fresh water which is at a constant temperature. This means that the streams can at best exit at the same temperature, which is that of the column of fresh water. As shown in Fig. 2(a), the water will exit the bubble column at a temperature that is much colder than that of the air inlet. The solution to this issue is to stack up multiple columns, each at a different temperature [6]. Figure 2(b) shows the effect of dividing an equal total coil length into 5 separate trays. The outlet of the saline water stream is much closer to the air inlet temperature when multiple columns are used. In fact, with enough columns, a multi-tray bubble column can reach very high values of energy effectiveness [13].

1.2. Improvements to the energy efficiency of HDH

Another issue that made early HDH systems less competitive was their relatively low energy efficiency, which prompted extensive research on the thermodynamics of HDH cycles. Mistry et al. [14, 15] found that the best efficiency was achieved when the entropy generation per unit mass of product was minimized and that most of the entropy generated in an HDH system was a result of the heat and mass transfer in the dehumidifier and the humidifier.

Some studies have looked at varying the water-to-air mass flow rate ratio throughout the system to decrease entropy generation. Müller-Holst [16, 17] cited the variability of the stream-to-stream temperature difference as a major source of entropy generation and suggested the continuous variation of the mass flow rate of air through extraction/injection to keep the stream-to-stream temperature difference constant throughout

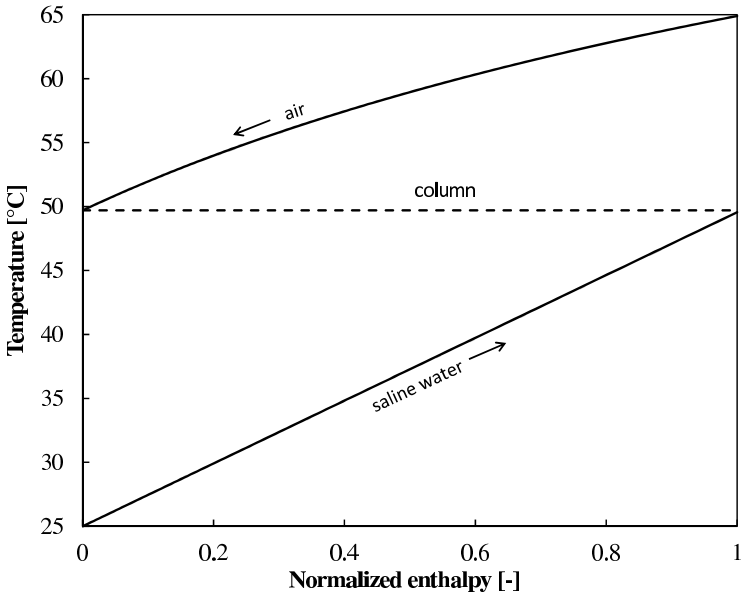

(a) Single-tray bubble column.

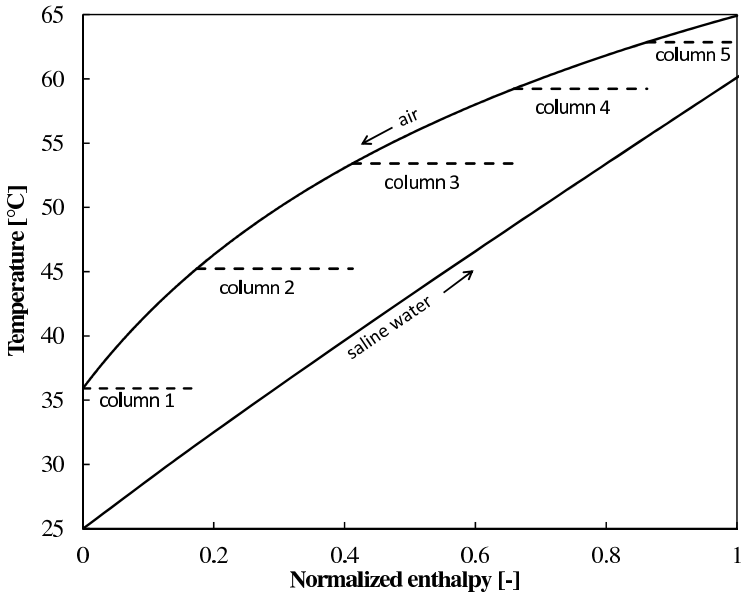

(b) Five-tray bubble column.

Fig. 2: Comparison of the performance of a single-tray bubble column and a five-tray bubble column. Both dehumidifiers have the same size, and operate under the same conditions. In the multi-tray dehumidifier, the coil length is divided equally between the trays [13].

the system. Zamen et al. [18] modeled a multi-stage system with each stage operating at a different water-to-air mass flow rate ratio. The model fixed a temperature pinch and used up to four stages. McGovern et al. [19] used temperature-enthalpy diagrams to represent the process paths of the water and air streams. They studied the variation of the performance of the system with the pinch point temperature difference and with the implementation of a single water extraction.

Thiel and Lienhard [20] showed that a larger portion of the entropy generation in the dehumidifier is a result of the mass transfer by diffusion due to the presence of high concentrations of air. This led to the conclusion that it is more important to balance the humidity ratio difference than the temperature difference. Narayan et al. [21] defined a modified control-volume based heat capacity rate ratio, HCR, and found that the entropy generation per unit water produced in a heat and mass exchanger with fixed inlet conditions and energy effectiveness was minimized at HCR = 1. Narayan et al. [22] expanded on that finding by defining an enthalpy pinch and suggesting that it was the correct pinch to balance at the two ends of a heat and mass exchanger as it takes into account the transfer of both heat and mass. They modeled systems without extraction, with a single air extraction, and with continuous extraction using a fixed enthalpy pinch model. Similarly, Chehayeb et al. [23] used a fixed enthalpy pinch model to study the performance of systems with up to 5 extractions/injections. In an experimental study, Narayan et al. [24] increased the energy efficiency of a system of fixed size by 54% by using a single air extraction.

In addition, Miller et al. [25] fixed the effectiveness of the humidifier and dehumidifier and varied the amount extracted in either direction and saw positive effects in some cases. Thiel et al. [26] used transport models of a packed-bed humidifier coupled with a tube-in-tube dehumidifier to study the effect of an extraction on the performance of a fixed-area system. They found that a water extraction from the dehumidifier to the humidifier could be beneficial with certain boundary conditions.

1.3. Purpose of this study

Most of the previous studies modeling HDH have evaluated the performance of the heat and mass exchangers by fixing their pinch or their effectiveness. These models have enhanced our understanding of the sources of entropy generation in HDH as discussed in the previous section; but, while they are very useful in predicting the performance of an HDH system under fixed operating conditions, they cannot be used to compare different operating conditions for a given system because pinch and effectiveness are strong functions of the flow rates of the streams in the system. For example, when an extraction/injection is used to vary the operation of an HDH system, the effectiveness and pinch in each component will change and only the physical sizes of the components remain constant. In addition, it is difficult to translate the results of fixed pinch or effectiveness models into practical recommendations, since the sizes of the exchangers used are not

specified.

Getting a complete picture of the balancing of HDH requires fixing the size of the system and using transport models to evaluate the performance of its components. In this study, we model an HDH system consisting of a packed-bed humidifier and a multi-tray bubble column dehumidifier. We study the effect of the mass flow rate ratio on the performance of the system and interpret that effect by looking at the specific entropy generation in each component as well as averages and variances of the driving forces in the humidifier and dehumidifier. In addition, we define a generalized effectiveness for heat and mass exchangers.

Further, we implement an air extraction/injection and simulate all possible operating points that do not result in a temperature mismatch between the injected stream and the main stream at the location of injection in the dehumidifier. We define criteria for best system performance, and we study the effect of the division of available area between stages. We also present a thorough explanation of why the direction of extraction should always be from the humidifier to the dehumidifier.

2. Modeling

In this section, we describe the models used to evaluate the performance of the different components of the system. These models were implemented in MATLAB and solved numerically. The details of the solution methods used can be found in Chehayeb et al. [13, 27] and will not be presented in this section. It is worth noting that each of these models was validated experimentally in previous studies [8, 28].

2.1. Multi-tray bubble column dehumidifier

As explained in Section 1.1, the use of bubble column dehumidifiers in HDH reduced the overall cost of the system and made it much more competitive. In this paper, we use the model established by Tow and Lienhard [8] to determine the performance of the bubble column dehumidifier. The model uses a resistance network to model the heat and mass transfer between the saline water in the coil and the moist air bubbles traveling through the column. It assumes perfect mixing in the column, which translates into having a negligible air-side resistance. The air therefore exits the column saturated at the temperature of the column. Tow and Lienhard [8] explain in detail why the air-side resistance is negligible, and verify the model experimentally for various conditions. This leaves us with two dominant resistances: the outer resistance, R_{out}, between the coil and the column of fresh water, which can be calculated using the correlation by Deckwer et al. [29], and the inner resistance, R_{in}, between the coil and the saline water, which is calculated using the correlation developed by Mori and Nakayama [30, 31] since the coil used is curved. The correlations for R_{out} and R_{in} are summarized in Appendix A.

A water mass balance on the bubble column yields the following equation:

$$\dot{m}_{\mathrm{cond,out}} = \dot{m}_{\mathrm{cond,in}} + \dot{m}_{\mathrm{da}} \left(\omega_{\mathrm{in}} - \omega_{\mathrm{out}}\right) \tag{1}$$

where $\dot{m}_{\mathrm{cond}}$ is the mass flow rate of the condensate, $\dot{m}_{\mathrm{da}}$ is that of dry air, and ω is the humidity ratio. We note that some condensate, $\dot{m}_{\mathrm{cond,in}}$, enters the tray in question from the previous, hotter tray, and the condensate leaving the tray, $\dot{m}_{\mathrm{cond,out}}$, enters the following, colder tray. In addition, the energy balance can be written as

$$\dot{m}_{\mathrm{da}} \left(h_{\mathrm{a,in}} - h_{\mathrm{a,out}}\right) \; + \; \dot{m}_{\mathrm{cond,in}} h_{\mathrm{cond,in}} \; - \; \dot{m}_{\mathrm{cond,out}} h_{\mathrm{cond,out}} = \dot{m}_{\mathrm{w}} \left(h_{\mathrm{w,out}} - h_{\mathrm{w,in}}\right) \equiv \dot{Q} \tag{2}$$

where h_{a} is the specific enthalpy of moist air, h_{w} is that of saline water, and $\dot{Q}$ is the heat transferred to the saline water.

A logarithmic mean temperature difference is defined since the saline water exchanges heat with the fresh water in the column which is at fixed temperature

$$\Delta T_{\mathrm{lm}} = \frac{T_{\mathrm{w,out}} - T_{\mathrm{w,in}}}{\ln\left(\frac{T_{\mathrm{col}} - T_{\mathrm{w,in}}}{T_{\mathrm{col}} - T_{\mathrm{w,out}}}\right)} \tag{3}$$

where T_{col} is the temperature of the fresh water in the column. And the heat transferred to the saline water can be expressed as

$$\dot{Q} = \frac{\Delta T_{\mathrm{lm}}}{R_{\mathrm{in}} + R_{\mathrm{out}}} = \dot{m}_{\mathrm{w}} \left(h_{\mathrm{w,out}} - h_{\mathrm{w,in}}\right) \tag{4}$$

The same equations can then be used to model a multi-tray bubble column with the additional step of matching the boundary conditions between consecutive trays. These equations can be solved without the need for simultaneous equations solvers by using the numerical solution algorithms developed by Chehayeb et al. [13, 27].

2.2. Packed-bed humidifier

A packed-bed humidifier is a cooling tower that serves to heat and humidify the moist air stream rather than cool the water as is common in power plants. Due to the wide use of cooling towers, we can model the packed-bed humidifier fairly accurately. In this paper, we use the most thorough model, namely the Poppe and Rögener model [32]. Kloppers and Kröger [33] present the equations used in that model as well as a numerical solution procedure based on the fourth-order Runge-Kutta method. Their approach was implemented in MATLAB and integrated with the rest of the system. The equations used are summarized

Table 1: Specifications of the system studied.

Operating conditions	
Top temperature, $T_{w,4}$	90 °C
Bottom temperature, $T_{w,1}$	25 °C
Feed mass flow rate, $\dot{m}_{w,in}$	0.242 kg/s
Feed water salinity	35 ppt
Humidifier geometry	
Height, H	3 m
Cross-sectional area	0.05 m^2
Fill surface area, a	226 m^2/m^3
Merkel number, Me	$0.967\left(\frac{\dot{m}_w}{\dot{m}_a}\right)^{-0.779} \times (3.28\ H)^{0.632}$
Minimum-maximum water loading	13.4-32 m^3/hr-m^2
Dehumidifier geometry	
Pipe length per tray	2.5 m
Number of trays, N_t	30
Pipe outer/inner diameter	9.5 mm/8.7 mm
Coil diameter	0.4 m

in Appendix B. For further details on the solution method the reader should refer to Klopper's doctoral thesis [28] as well as Chehayeb et al. [13, 27]. The model uses parameters for the CF-1200MA packing from Brentwood Industries, whose properties are summarized in Table 1.

2.3. Single-stage HDH system

A humidification dehumidification system without extraction/injection can be modeled by coupling a humidifier and a dehumidifier and matching the air temperature between the two components. For additional details on implementing the numerical solution algorithm for the complete system the reader can refer to Chehayeb et al. [13, 27].

2.4. Two-stage HDH system

It has previously been proven than varying the water-to-air mass flow rate ratio can improve the performance of the system [19, 22, 23]. Having modeled each component in the system separately, the algorithm used in modeling a system with a single extraction consists of matching the boundary conditions between the different components. Numerically this is not as straightforward as the algorithm for a system without extraction due to the fact that we now have two air flow rates to vary. What makes the modeling even more challenging is the fact that the two stages in the system are very interdependent. We cannot think of each stage as a system that can be solved separately since the intermediate temperatures are determined by the flow rates chosen in each of the stages. In other words, varying the mass flow rate of air in the top stage while keeping the flow rate of air constant in the bottom stage will change the intermediate temperatures in the system, affecting the lower stage.

In modeling a system with a single extraction, the sizes of the dehumidifier and the humidifier, the top and bottom temperatures, and the feed flow rate are fixed. We can vary the locations of the extraction and the injection, as well as the flow rates of air in the two stages.

If we treat both flow rates of dry air as variables, most of the resulting cases will have a temperature mismatch between the injected stream and the main stream in the dehumidifier at the location of injection. To reduce the number of possible operating points, we only consider the cases in which the temperature of the injected stream is exactly equal to that of the main stream in the dehumidifier at the location of injection. This leaves us with three variables: the pair of dry air flow rates, the location of extraction, and the location of injection.

In addition, in each stage, the heat duty in the humidifier is the same as that in the dehumidifier because the air runs in a closed loop and its temperatures are matched at the terminal locations:

$$\dot{Q}_{\mathrm{duty,h,1}} = \dot{Q}_{\mathrm{duty,d,1}} = \dot{H}_{\mathrm{a,2}} - \dot{H}_{\mathrm{a,1}} \tag{5}$$

$$\dot{Q}_{\mathrm{duty,h,2}} = \dot{Q}_{\mathrm{duty,d,2}} = \dot{H}_{\mathrm{a,3}} - \dot{H}_{\mathrm{a,2}} \tag{6}$$

$$\dot{Q}_{\mathrm{duty,h,1}} + \dot{Q}_{\mathrm{duty,h,2}} = \dot{Q}_{\mathrm{duty,d,1}} + \dot{Q}_{\mathrm{duty,d,2}} = \dot{Q}_{\mathrm{duty}} \tag{7}$$

$$\frac{\dot{Q}_{\mathrm{duty,h,1}}}{\dot{Q}_{\mathrm{duty}}} = \frac{\dot{Q}_{\mathrm{duty,d,1}}}{\dot{Q}_{\mathrm{duty}}} \tag{8}$$

where 'a,1', 'a,2', and 'a,3' denote the locations along the air stream shown in Fig. 1. $\dot{Q}_{\mathrm{duty}}$ is the total heat duty in the system, and $\dot{Q}_{\mathrm{duty,h,1}}$ is the heat duty in the humidifier of the first stage, denoted by 'Humidifier 1' in Fig. 1.

Given that the heat and mass transfer coefficients do not change greatly along the length of either component, Eq. 8 can also result in the requirement that the division of area between the hot and cold stage be the same in the humidifier and dehumidifier:

$$\frac{H_1}{H} = \frac{N_{\mathrm{t,1}}}{N_{\mathrm{t}}} \tag{9}$$

where H is the total height of the packed-bed humidifier, H_1 is the height of the humidifier of the first stage, N_{t} is the total number of trays in the dehumidifier, and $N_{\mathrm{t,1}}$ is the number of trays in the dehumidifier of the first stage. This requirement replaces the variables of location of extraction and location of injection by one variable which is the fraction of the total area allocated to the first stage.

To find the pair of mass flow rates of dry air that would result in no temperature mismatch at the location of injection, we specify the intermediate water temperature in the dehumidifier, $T_{w,2}$, shown in Fig. 1. Fixing $T_{\mathrm{w,2}}$ allows us to model the top stage as a system without extraction with fixed top and bottom temperatures

as described in Section 2.3. Once $T_{w,2}$ is picked, we have to determine the air flow rate in the top stage, $\dot{m}_{da,2}$, which results in no temperature mismatch at the location of injection. We can set reasonable bounds on the mass flow rate ratio in the top stage from the results presented in [22, 23]. After picking the flow rate of air in the top stage, we can calculate $T_{a,2}, T_{a,3}, T_{w,3}$, and $T_{w,5}$.

In the dehumidifier of the first stage, the water inlet and outlet temperatures, and the top air temperature are known. We can find the appropriate flow rate of air that, given the inlet temperatures, would result in the desired $T_{w,2}$. By finding the appropriate $\dot{m}_{da,1}$, we also find $T_{a,1}$.

Finally, in the humidifier of the first stage, the water and air inlet temperatures and flow rates are known so we can calculate the outlet temperatures: $T_{w,6}$ and $T_{a,2,b}$. Note the added subscript 'b' since this calculated temperature is not necessarily equal to $T_{a,2}$ calculated in the second stage. Knowing that these two temperatures must be equal, we can vary $\dot{m}_{da,2}$ as explained in greater detail in Fig. D.15 in Appendix D.

2.5. Performance parameters

To evaluate the performance of the system under different operating conditions, we look at two parameters. The first parameter is the gained output ratio, GOR, which is commonly used in thermal desalination technologies as a measure of energy efficiency. It is defined as the ratio of the latent heat of vaporization to the net heat input into the system:

$$\mathrm{GOR} = \frac{\dot{m}_{pw} h_{fg}}{\dot{Q}_{in}} \tag{10}$$

GOR is then a dimensionless quantity which quantifies how well the heat input is reused. As explained is Section 1, the reuse of heat is done by using the heat of condensation to preheat the feed saline water in the dehumidifier before it enters the heater. The best a system can achieve without reusing the heat of condensation is then a GOR of 1. In this paper we evaluate the latent heat of vaporization, h_{fg}, at 50 °C and 35 ppt.

Another important measure of performance is the recovery ratio, RR, which is the ratio of the rate of pure water production to the rate of feed entering the system:

$$\mathrm{RR} = \frac{\dot{m}_{pw}}{\dot{m}_{w}} \tag{11}$$

In this analysis, as we are keeping the feed flow rate constant, RR is also a direct measure of absolute water production.

3. Effect of the mass flow rate ratio on the performance of a single-stage system

The results presented in this paper are divided into two parts: a first part that studies the effect of the mass flow rate ratio on the performance of a single-stage system, and a second part that deals with the implementation of a single air extraction/injection.

In the following results, we simulate a system of fixed size whose specifications are summarized in Table 1. The water-to-air mass flow rate ratio is varied by changing the flow rate of dry air while keeping the feed flow rate constant. Each point in the results corresponds to a value of the water-to-air mass flow rate ratio between 3 and 20 (with increments of 0.2).

3.1. Definition of the modified heat capacity rate ratio, HCR

As explained in Section 1.2, the modified heat capacity rate ratio was first defined by Narayan et al. [21] as the ratio of the maximum changes in enthalpy rates of the interacting streams in a heat and mass exchanger:

$$\mathrm{HCR} = \frac{\Delta \dot{H}_{\mathrm{max,cold}}}{\Delta \dot{H}_{\mathrm{max,hot}}} \tag{12}$$

In a heat exchanger, Eq. 12 reduces to the well-known definition of the heat capacity rate ratio. This can be done since the specific heat capacities of the streams do not vary greatly and the maximum change in temperature that both streams can experience is the same and cancels out:

$$\mathrm{HCR_{HE}} = \frac{(\dot{m}c_p)_{\mathrm{cold}}}{(\dot{m}c_p)_{\mathrm{hot}}} \tag{13}$$

In a heat and mass exchanger, however, the specific heat of at least one of the two streams can vary greatly. In the case of HDH, the specific heat of moist air includes the latent heat of water vapor which means it is a strong function of the absolute temperature. As a result, the definition of HCR does not reduce to that used in a heat exchanger.

As will be apparent in the following sections, a parameter of great importance for the performance of HDH is the heat capacity rate ratio in the dehumidifier, $\mathrm{HCR_d}$, which can be expressed as:

$$\mathrm{HCR_d} = \frac{\dot{m}_{\mathrm{w}}}{\dot{m}_{\mathrm{da}}} \times \frac{\left(h_{\mathrm{w}}|_{T_{\mathrm{a,in}}} - h_{\mathrm{w}}|_{T_{\mathrm{w,in}}}\right)}{\left(h_{\mathrm{a}}|_{T_{\mathrm{a,in}}} - h_{\mathrm{a}}|_{T_{\mathrm{w,in}}}\right) \; - \; \left(\omega|_{T_{\mathrm{a,in}}} - \omega|_{T_{\mathrm{w,in}}}\right) h_{\mathrm{cond}}|_{T_{\mathrm{w,in}}}} \tag{14}$$

Figure 3 represents the process paths of the water and moist air streams in a single-stage HDH system on a temperature-enthalpy diagram. As suggested by McGovern et al. [19], the enthalpy is expressed per unit dry air so that all the process paths can be superposed on the same graph. Equation 12 can also be

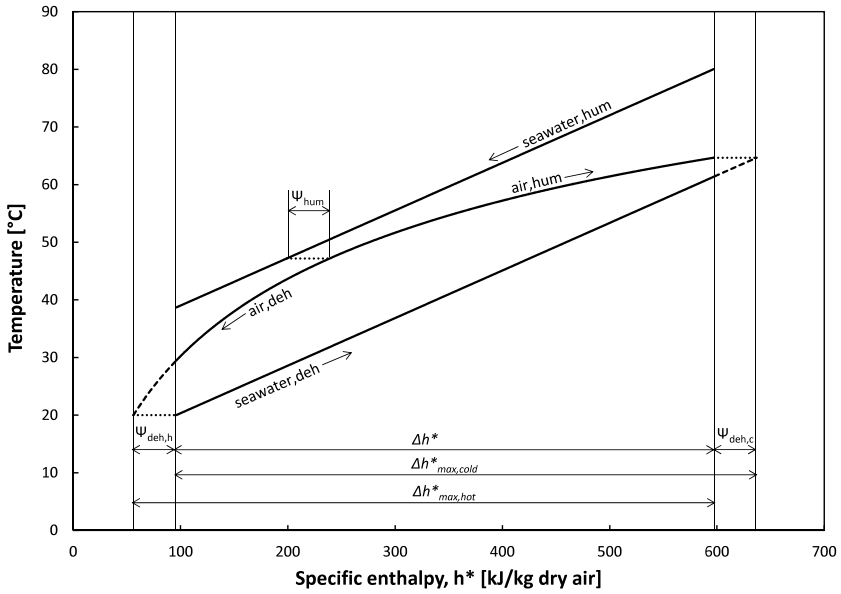

Fig. 3: Temperature-enthalpy profile of a balanced single-stage system with $T_{\text{feed}} = 20\,^{\circ}\text{C}$, $T_{\text{top brine}} = 80\,^{\circ}\text{C}$, and $\Psi_{\text{hum}} = \Psi_{\text{deh}} = 20$ kJ/kg dry air [23].

expressed in enthalpy per unit dry air by dividing the numerator and denominator by the mass flow rate of dry air:

$$\text{HCR} = \frac{\Delta h^*_{\text{max,cold}}}{\Delta h^*_{\text{max,hot}}} = \frac{\Delta h^* + \Psi_{\text{deh,c}}}{\Delta h^* + \Psi_{\text{deh,h}}} \tag{15}$$

where Ψ is the enthalpy pinch, defined by Narayan et al. [22] as the loss in enthalpy rate (per unit mass of dry air) as a result of having a finite exchanger size. This allows us to better visualize the definition of HCR_{d} in Fig. 3.

3.2. Optimal performance of a single-stage system

Figure 4(a) shows the variation of the energy efficiency of the system represented by the gained output ratio, GOR, with the modified heat capacity rate ratio in the dehumidifier, HCR_{d}. It can clearly be seen that the best energy efficiency is achieved at $\text{HCR}_{\text{d}} = 1$, or when the maximum change in the enthalpy rate is equal between the two interacting streams in the dehumidifier. This result is consistent with the fixed-effectiveness model reported by Narayan et al. [21]. In addition, we can also see in Fig. 4(b) that the water production is also maximized when $\text{HCR}_{\text{d}} = 1$.

Equation 16 links the heat duty to the heat input into the system. This is done by applying an energy balance on the feed stream from the inlet of the dehumidifier to the inlet of the humidifier. In that control volume, some heat is added in the dehumidifier by recovering the heat of condensation, denoted by $\dot{Q}_{\text{duty}}$, and the remaining energy required to reach the top temperature is added in the heater, denoted by $\dot{Q}_{\text{in}}$. In the system studied, the top and bottom temperatures are fixed, so the total heat input to the seawater

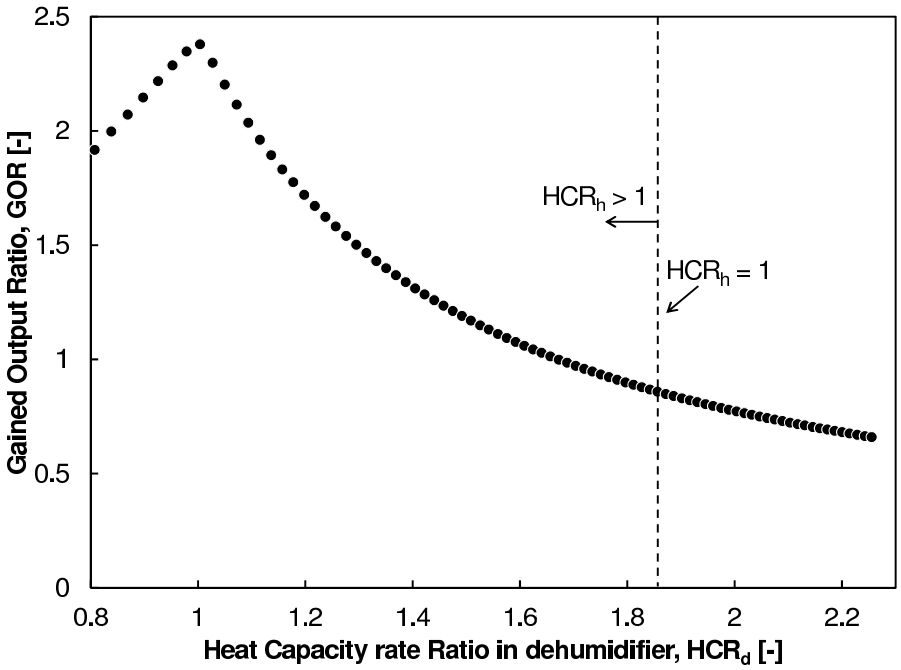

(a) Variation of GOR with HCR_d.

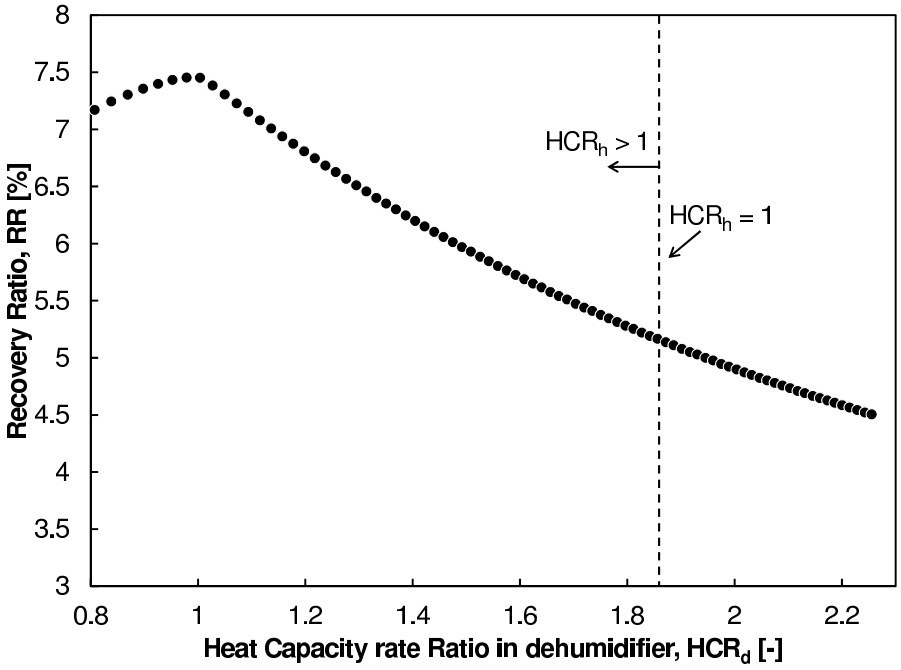

(b) Variation of RR with HCR_d.

Fig. 4: Variation of the performance of a single-stage HDH system with HCR_d.

stream required to take it from the bottom temperature to the top temperature is fixed:

$$\dot{m}_{\mathrm{w,in}}\left(h_{\mathrm{w},4}-h_{\mathrm{w},1}\right)=\dot{Q}_{\mathrm{duty}}+\dot{Q}_{\mathrm{in}}=\text{constant} \tag{16}$$

Equation 16 can be used to explain why the gained output ratio and the recovery ratio vary in the same manner. GOR can be increased by decreasing $\dot{Q}_{\mathrm{in}}$, which is done by increasing the heat duty. The larger the heat duty, the larger the flow rate of moist air, and/or the wider the range between the bottom and top air temperatures. Both of these consequences translate into a higher water production in the system. Therefore, a higher heat duty results in higher water production in addition to better energy efficiency.

This means that by fixing the size of the system, the top and bottom temperatures, and the feed flow rate, there is only one flow rate of air, or one mass flow rate ratio, that maximizes both the energy efficiency and the water production. We can operate the system under different feed flow rates, but for each of these flow rates there is only one flow rate of air that results in optimal performance in terms of both energy efficiency and water production. As we increase the feed flow rate, the water production rate will increase but the energy efficiency will drop because the area per unit flow will decrease and so will the effectiveness of the exchangers. The trade-off between the different values of the feed flow rate is then between energy efficiency and water production. Assessing that trade-off requires a cost analysis and is beyond the scope of this paper.

3.3. Interpretation of $HCR_d = 1$.

To understand why $\mathrm{HCR_d}$ is an important parameter when looking at the energy efficiency of the system we consider the entropy generated per unit product. Figure 5 shows the entropy generated in the dehumidifier and the humidifier separately and collectively for different values of the mass flow rate ratio. It can be seen that the total entropy generated is minimized at $\mathrm{HCR_d} = 1$, which explains why we get the best energy efficiency at that mass flow rate ratio. This result is consistent with the conclusion by Mistry et al. [34] that the best performance is achieved when the specific entropy generated is minimized.

We can also see that the entropy generated in the dehumidifier is always larger than that generated in the humidifier, which is almost independent of $\mathrm{HCR_d}$. Further, the entropy generated in the dehumidifier is minimized at $\mathrm{HCR_d} = 1$ whereas the entropy generated in the humidifier shows no change in trend around $\mathrm{HCR_h} = 1$. The effect of $\mathrm{HCR_h}$ is discussed in greater detail in Section 3.4. What can be concluded from this graph is that the variation of the mass flow rate ratio affects the entropy generated in the dehumidifier much more strongly than that generated in the humidifier, as evident by the slopes of the two curves in Fig. 5, which is why $\mathrm{HCR_d}$ is the parameter to monitor when thermodynamically balancing a single-stage HDH system. In fact, balancing the dehumidifier from a control volume perspective has little negative effect on the humidifier, and therefore serves to maximize the performance of the system.

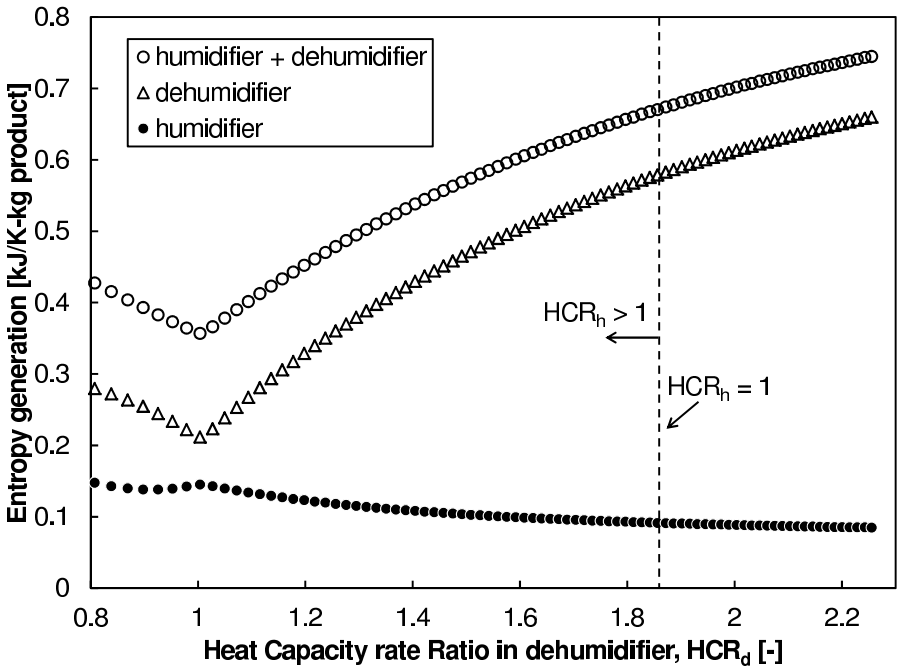

Fig. 5: Variation of entropy generation with $\mathrm{HCR_d}$.

In a heat and mass exchanger, entropy generation can be ascribed to two factors: (1) a finite mean driving force for heat and mass transfer, and (2) a spatial or temporal variance in the driving force [35]. The size of the system affects mainly the mean driving force whereas the mass flow rate ratio affects mostly the variance of the driving force. In this study, in order to better show the effect of the mass flow rate ratio, we model a very large system ($\varepsilon_\mathrm{d} \approx 99\%$, $\varepsilon_\mathrm{h} \approx 95\%$). In a larger system, the total entropy generation is smaller; and the entropy generation due to the variance of the driving forces forms a greater fraction of the total entropy generation, which makes the effect of balancing more pronounced. In addition, we have also simulated smaller systems and found that GOR and RR are maximized at $\mathrm{HCR_d} = 1$, and that the specific entropy generation is also minimized at the same mass flow rate ratio.

We can also look at the effect of the mass flow rate ratio on the driving forces for heat and mass transfer. The averages and variances in this study are weighted spatially using the surface area. Figure 6(a) shows the variation of the average driving force for heat transfer, namely the temperature difference between the two interacting streams in the humidifier and the dehumidifier. We can clearly see that the average temperature difference in both the humidifier and dehumidifier is maximized at $\mathrm{HCR_d} = 1$, which means that, given a fixed exchanger size and relatively fixed heat transfer coefficients, the highest heat duty is achieved at $\mathrm{HCR_d} = 1$. For smaller systems, the curves shown in Fig. 6(a) become much flatter, and the peak in the dehumidifier remains at $\mathrm{HCR_d} = 1$ whereas that in the humidifier shifts to $\mathrm{HCR_d}$ slightly larger than 1.

Figure 6(b) shows the variation of the average difference in relative humidity in both the humidifier and

dehumidifier. The difference is taken between the humidity ratio of air and the humidity ratio at saturation evaluated at the temperature and salinity of the water at multiple locations along the exchangers. The average difference in the humidity ratio in the dehumidifier is maximized whereas that in the humidifier is close to its maximum at $\mathrm{HCR_d} = 1$. The same trends can be seen in systems of smaller size.

Figure 7 shows the variation of the variances of the stream-to-stream temperature and humidity ratio differences with $\mathrm{HCR_d}$. At $\mathrm{HCR_d} = 1$, the variance of the temperature difference in the dehumidifier is minimized and that in the humidifier is close to its minimum. In addition, the variance of the humidity ratio difference in the dehumidifier is minimized and only the variance of the humidity ratio difference in the humidifier is not at a minimum at $\mathrm{HCR_d} = 1$. For smaller systems, the trends in the variances in the humidifier remain the same. In the dehumidifier, the minimum variance of the temperature difference shifts to $\mathrm{HCR_d}$ slightly larger than 1 whereas the variance of the humidity ratio difference shifts to $\mathrm{HCR_d}$ less than 1. Balancing the two driving forces can be done by operating the system around $\mathrm{HCR_d} = 1$.

Minimizing the variance of the driving force means that it remains as close as possible to its average along the heat and mass exchanger. This in turn means that the driving force will not become too large at some points and too small at other points, which means that all of the available exchanger surface area is used fully. If the heat and mass exchanger is not balanced properly, the stream with the smaller total heat capacity rate will quickly reach a state close to that of the other stream, and the rest of the available area will only result in a small heat duty because the driving force is too small. This result is consistent with the conclusion reached by Thiel et al. [35] that the best performance is obtained by minimizing the variance of the driving force.

3.4. A modified definition of the effectiveness of heat and mass exchangers

Narayan et al. [36] defined the effectiveness of a heat and mass exchanger as:

$$\varepsilon = \frac{\Delta \dot{H}}{\Delta \dot{H}_{\mathrm{max}}} \tag{17}$$

where they define $\Delta \dot{H}_{\mathrm{max}}$ as the minimum of the maxima that be achieved by the two streams:

$$\Delta \dot{H}_{\mathrm{max}} = \min\left(\Delta \dot{H}_{\mathrm{max,cold}}, \Delta \dot{H}_{\mathrm{max,hot}}\right) \tag{18}$$

The maximum change in the enthalpy rate of each stream is that which occurs if that stream exits at the inlet state of the other stream. Only the smaller of these maxima can occur as dictated by an energy balance.

This definition of the maximum change in enthalpy rate is accurate when dealing with a heat and mass exchanger such as the dehumidifier in an HDH system where the pinch always occurs at a terminal location,

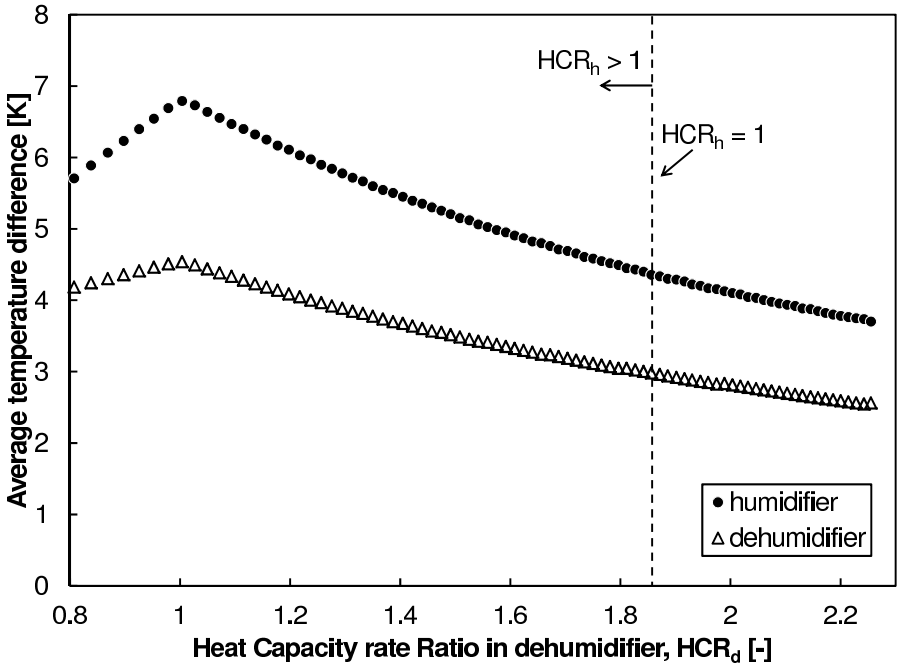

(a) Variation of the average of the stream-to-stream temperature difference with HCR_d.

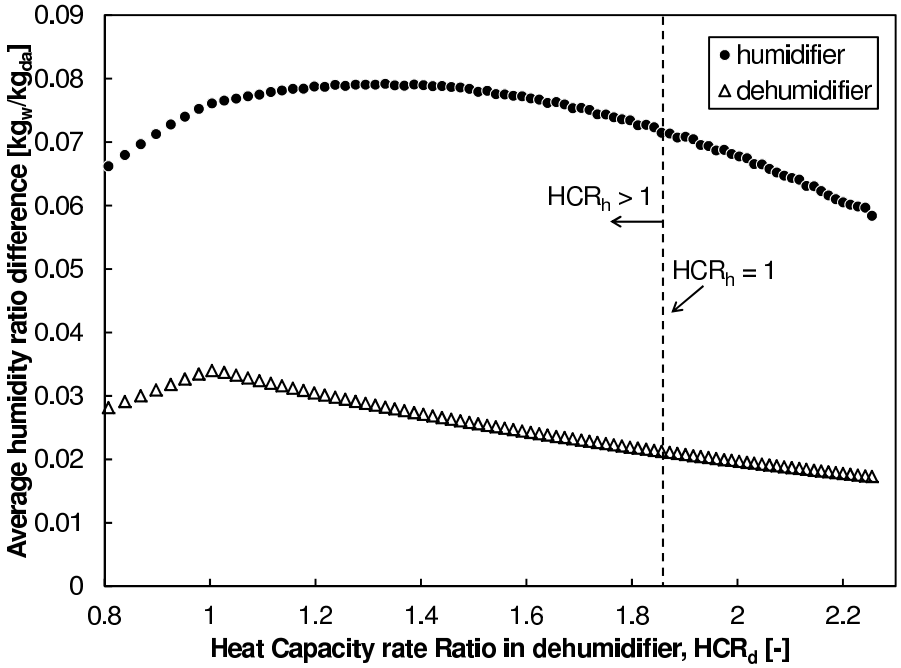

(b) Variation of the average of the stream-to-stream humidity ratio difference with HCR_d.

Fig. 6: Variation of the average of the driving forces with HCR_d.

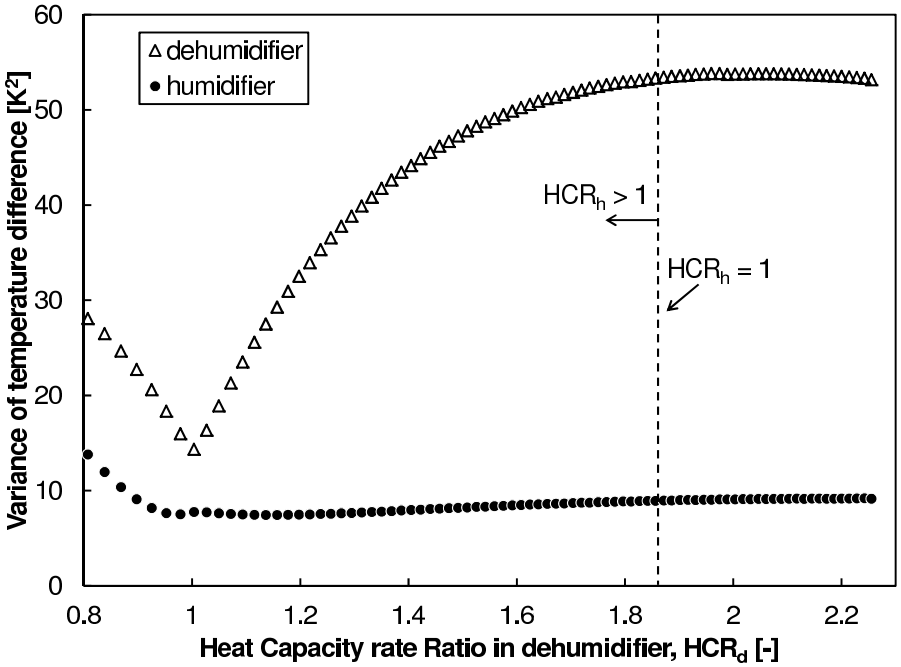

(a) Variation of the variance of the stream-to-stream temperature difference with HCR_d.

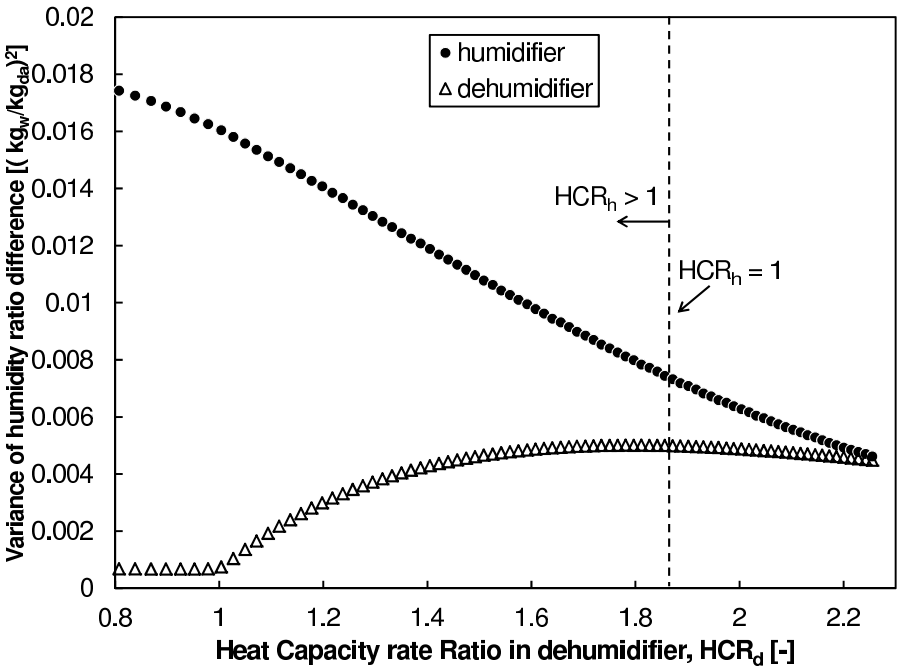

(b) Variation of the variance of the stream-to-stream humidity ratio difference with HCR_d.

Fig. 7: Variation of the variance of the driving forces with HCR_d.

as can be seen in Fig. 3. This means that with an effectively infinite dehumidifier at least one of the two streams will exit the exchanger at equilibrium with the inlet of the other stream. In the humidifier, however, the pinch point occurs at an intermediate location rather than at the terminals (except for extreme values of the mass flow rate ratio). This behavior is due to the shape of the saturation curve as well as to the moist air being the colder stream, as opposed to the dehumidifier where the air is the hotter stream, as shown in Fig. 3. Having an effectively infinite humidifier will result in an intermediate pinch equal to zero, which means that neither of the streams can reach the inlet state of the other stream without resulting in a temperature cross. Therefore, the maxima determined by considering each stream separately cannot be achieved even with an infinitely large exchanger.

This prompts us to redefine the denominator of the effectiveness of the humidifier, or similar heat and mass exchangers where the pinch occurs at an intermediate location, by using a more general definition: the maximum change in the enthalpy rate is that achieved when the heat and mass exchanger has a zero pinch, regardless where that pinch occurs:

$$\varepsilon = \frac{\Delta\dot{H}}{\Delta\dot{H}_{\max}} = \frac{\Delta\dot{H}}{\Delta\dot{H}|_{\text{pinch}=0}} \tag{19}$$

The exact definition of effectiveness of a humidifier can only be calculated by simulating an exchanger of effectively infinite area since the flow rate of water will change due to the increased evaporation rate as the exchanger becomes larger. However, as a good approximation, for the humidifier in an HDH system we can calculate the effectiveness as

$$\varepsilon_{\text{h}} \approx \frac{\Delta\dot{H}}{\Delta\dot{H} + \dot{m}_{\text{da}}\Psi_{\text{hum}}} \tag{20}$$

where Ψ_{hum} is the enthalpy pinch in the humidifier as shown in Fig. 3. This approximation is a result of assuming that the additional evaporation due to the increased exchanger size will not have a significant effect on the flow rate of water, and the pinch point will occur at the point of tangency between the two curves. The maximum change in enthalpy rate that can be achieved by using an effectively infinite exchanger is the sum of the change in enthalpy rate at finite size, $\Delta\dot{H}$, and the change in enthalpy rate lost due to having finite surface area, $\dot{m}_{\text{da}}\Psi_{\text{hum}}$.

In addition, the previous definition of effectiveness was limited by a maximum value that is less than one. This meant that setting the effectiveness of a component higher than the maximum value would result in a temperature cross, which violates the Second Law of Thermodynamics. The generalized definition proposed above will never result in such cases since the denominator in Eq. 19 is the value of the change in enthalpy rate that can be achieved at zero pinch. An effectiveness less than one, by definition, guarantees a positive pinch.

Further, the new definition is a better performance parameter for heat and mass exchangers as it compares

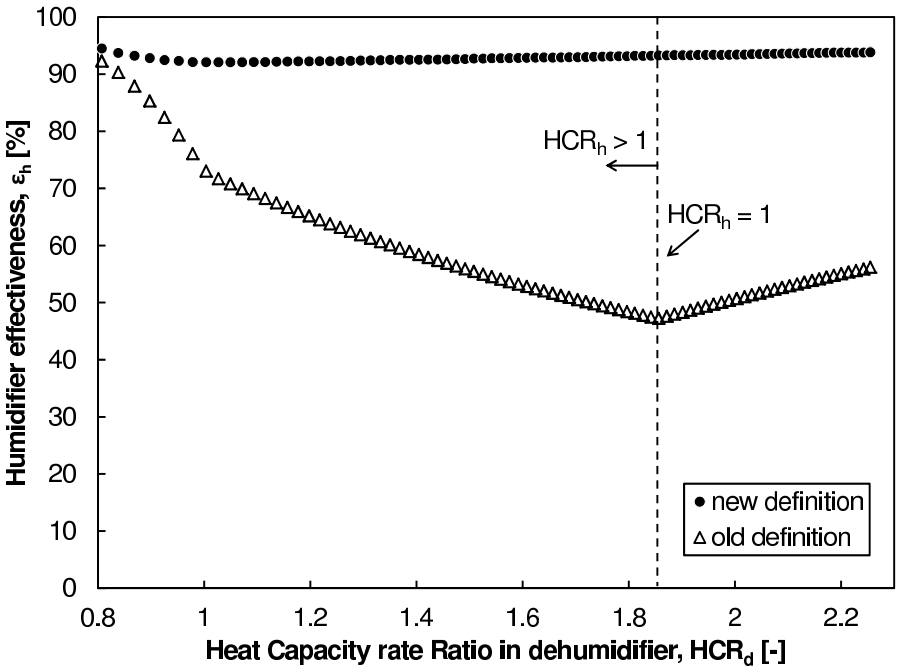

Fig. 8: Comparison of the old and new definitions of humidifier effectiveness.

their current performance to the best that can be achieved. Figure 8 shows the variation of the new and old definitions of effectiveness of the humidifier with HCR_d. Using the old definition to calculate an effectiveness of 50% is misleading as the designer would think that the exchanger is too small and the performance could be twice as good with an infinitely large exchanger. In reality, with the prior definition the performance is being compared to one that can never be achieved; and, by using the new definition, the same operating point would have an effectiveness of 90% as seen in Fig. 8, which means much less performance can gained by increasing the size of the component. Also, we can see that the effectiveness of the humidifier is not a strong function of the mass flow rate ratio as the pinch occurs at an intermediate location. The two definitions of effectiveness meet at extreme values of the mass flow rate ratio where the pinch in the humidifier occurs at one of the terminals.

Defining a new maximum change in enthalpy rate explains why HCR_h, which is the ratio of the maximum changes of enthalpy rate of the two streams, is not an important parameter for an HDH system. Having stream maxima that cannot be achieved even at 100% effectiveness renders their ratio meaningless. For this reason, HCR_h is not a useful parameter for balancing an HDH system. This can clearly be seen in Fig. 4, 5, 6, 7, and 8 where $HCR_h = 1$ does not result in any extrema in the parameters studied, even those strongly dependent on the humidifier.

4. Implementing a single air extraction/injection

As explained in Section 2.4, the sizes of the components and the top and bottom temperatures are fixed at the values listed in Table 1. Each different operating point presented in the results of this section corresponds to a specified location of extraction/injection (represented by the division of the area between the two stages) and a specified value of the intermediate temperature of the water in the dehumidifier, $T_{w,2}$.

The number of trays in the first stage, $N_{t,1}$, is varied between 3 and 24, with $N_t = 30$. For example, if we set $N_{t,1} = 12$, this means $N_{t,2} = N_t - N_{t,1} = 18$. The available area in the humidifier ($H = 3$ m) is divided in the same proportions: $H_1 = H \times \frac{N_{t,1}}{N_t} = 1.2$ m, and the rest of the available humidifier height is in the second stage. At each location, $T_{w,2}$ is varied, and the pair of mass flow rates of dry air that result in no temperature mismatch are calculated using the algorithm described in Section 2.4. $T_{w,2}$ is increased until the available area in the first stage is no longer sufficient to supply the appropriate heat duty.

The mass flow rate of dry air in the first stage required to heat the water to $T_{w,2}$ spikes at a certain $T_{w,2,max}$. This happens because as $T_{w,2}$ increases the mass flow rate of dry air in the second stages decreases, so it is possible to get an effectiveness of 100% in the dehumidifier of the second stage. With the air being the stream with the smaller heat capacity rate, the temperature of the extracted air stream, $T_{a,2}$, becomes equal to $T_{w,2}$. This in turn means that the dehumidifier of the first stage must have an effectiveness of 100% with the water being the stream with the smaller heat capacity rate. In order to heat the water up to the desired $T_{w,2} \approx T_{a,2}$, the mass flow rate of air must be increased until the area available is no longer enough to accommodate the heat and mass transfer required.

In simulating the system, extrema are imposed on the allowable values that the mass flow rates of dry air can take. In this simulation, the mass flow rate ratio was chosen between 1 and 40, which, as seen in Narayan el. [22], covers the full range of desirable ratios under which to operate.

4.1. Criteria for optimal performance in a two-stage system

This section studies the effect of the heat capacity rate ratio on the performance of the system, represented by the gained output ratio and the recovery ratio. We note that the data points are the same in Fig. 9(a), 9(b), and 10; however, to show the results clearly, the space is plotted in 3 different graphs. What is clear from Fig. 9(a) is that the point with the highest GOR has $HCR_{d,1} = 1$. In addition, Fig. 9(b) shows that that same point satisfies $HCR_{d,2} = 1$. Figure 10 represents the variation of GOR with both $HCR_{d,1}$ and $HCR_{d,2}$, and clearly shows that GOR is maximized when $HCR_{d,1} = HCR_{d,2} = 1$. Setting $HCR_{d,1} = HCR_{d,2} = 1$ in a two-stage HDH system means that both stages are thermodynamically balanced, which is consistent with the results presented in Section 3.2.

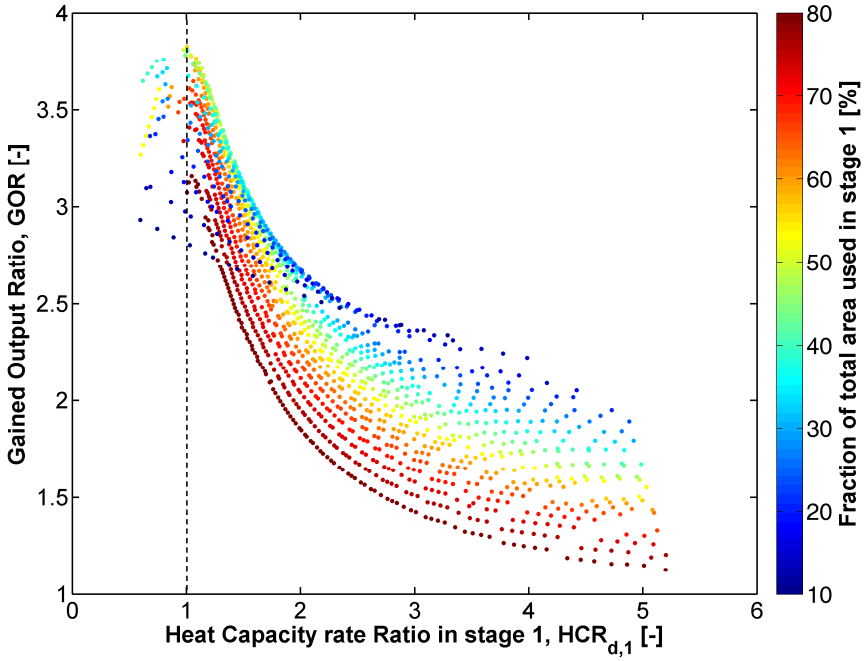

(a) Variation of GOR with $HCR_{d,1}$.

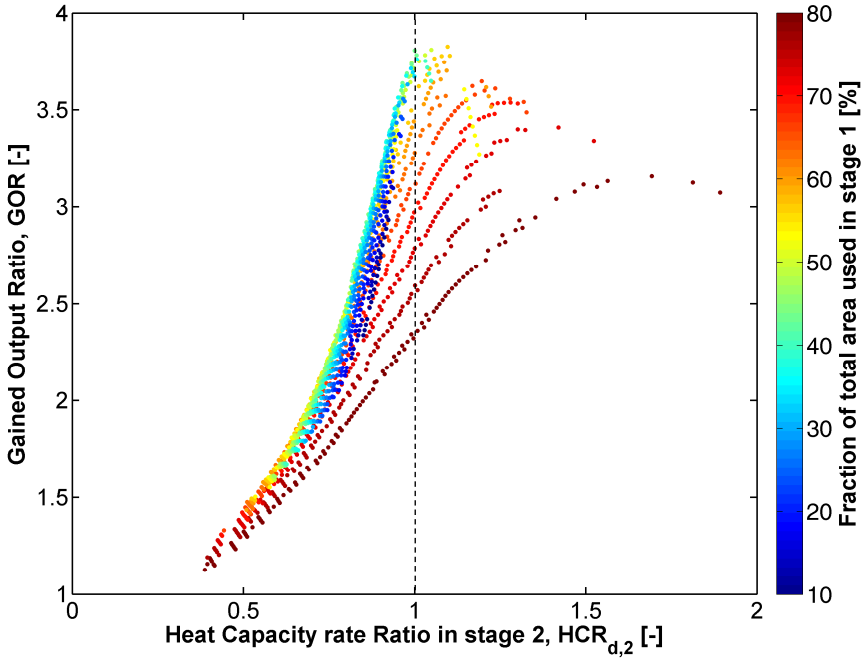

(b) Variation of GOR with $HCR_{d,2}$.

Fig. 9: Variation of GOR with $HCR_{d,1}$ and $HCR_{d,2}$.

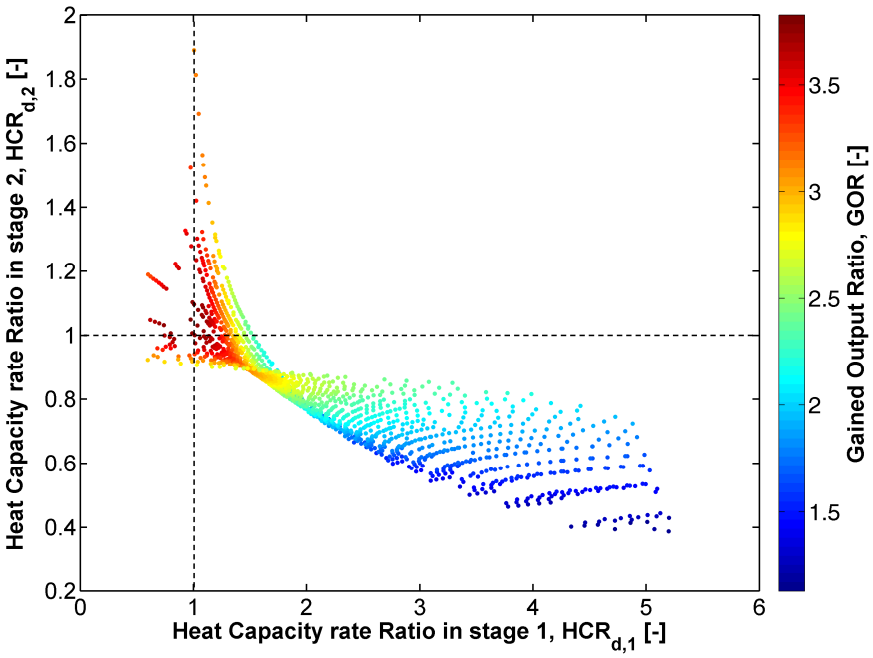

Fig. 10: Variation of GOR with $HCR_{d,1}$ and $HCR_{d,2}$.

Figure 11 shows the variation of GOR with recovery ratio. The points plotted are the same as those presented in Fig. 9 and 10. It can be clearly seen that GOR and RR vary in the same direction, meaning that optimizing the operation for energy efficiency will also maximize water production, which is consistent with the results presented in Section 3.2, where a thorough interpretation of the agreement is given.

The highest GOR that could be reached with this system size without any extraction/injection was 2.4, and this value was raised by 58% to 3.8 by using a single extraction. Similarly, the recovery ratio was increased from 7.4% to 8.2% as a result of the extraction/injection. The best performance in this case is achieved when the area is equally divided between the two stages. The effect of the location of extraction/injection is discussed in detail in the following section.

In addition to the results reported in Fig. 9 and 10 we also simulated a system where we treated the location of extraction in the humidifier as a separate variable, independent from that in the dehumidifier, and the results also showed maxima at $HCR_{d,1} = HCR_{d,2} = 1$. In this paper, however, we will only show the plots that treat both the location of extraction and the location of injection as one variable as they make it easier to to isolate the effect of the location of extraction/injection which is studied in the following section.

Finally, HCR_h remains an irrelevant parameter when balancing an HDH system even with the implementation of a single air extraction/injection. This is consistent with the results and interpretation presented in Section 3.4.

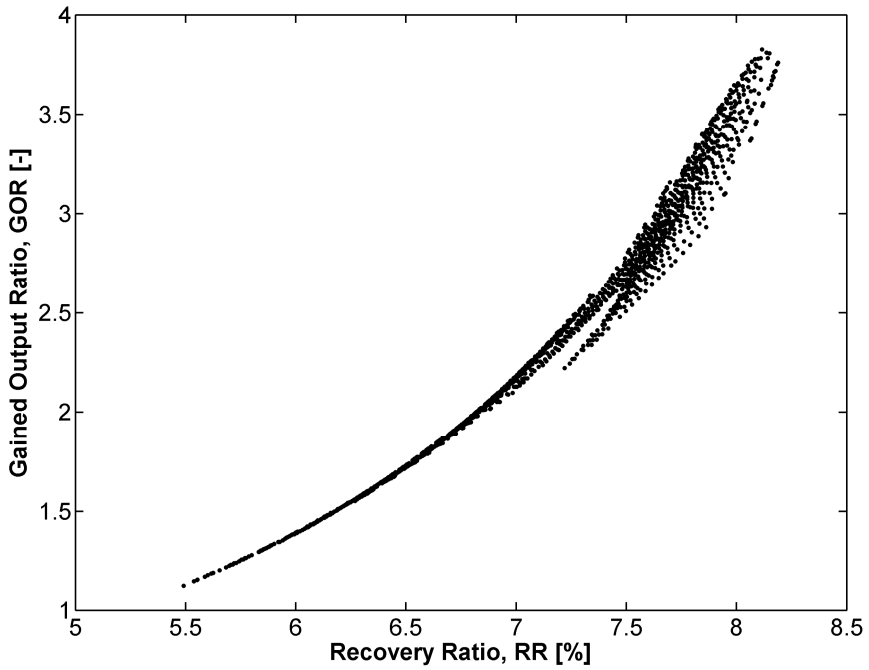

Fig. 11: Variation of GOR with RR.

4.2. Effect of location of extraction/injection on performance

Figure 12 shows the variation of $HCR_{d,1}$ and $HCR_{d,2}$ with the location of extraction/injection. As shown in Section 4.1, it is desired to operate with the mass flow rates of dry air that result in $HCR_{d,1} = HCR_{d,2} = 1$, and, as can be seen in Fig. 12, this is only possible at some of the locations of extraction, and possibly only at a single location of extraction. If only a small fraction of the total area is allotted to the first stage, we can see that this will result at best in $HCR_{d,1} = 1$ but will have $HCR_{d,2} < 1$. Similarly, if a very large area is allotted to the first stage, the best we can get is $HCR_{d,1} = 1$ with $HCR_{d,2} > 1$, or $HCR_{d,2} = 1$ with $HCR_{d,1} > 1$. In order to achieve complete balancing of the two stages as well as a matched injection temperature, we need to choose the appropriate location of extraction/injection. In this study, the highest GOR was achieved by equally dividing the area between the two stages, but one system size is not enough to make a conclusion regarding the exact relative location of the extraction.

The condition that the temperature of the injected stream has to be the same as that of the main stream in the dehumidifier just before the point of injection limits the number of possible flow rates of dry air that we can operate under, as explained in Section 2.4. If this constraint is relaxed and a temperature mismatch is allowed, we could treat each flow rate as a separate variable. This could result in more cases where $HCR_{d,1} = HCR_{d,2}$ but with some additional entropy generation due to the mixing at the point of injection.

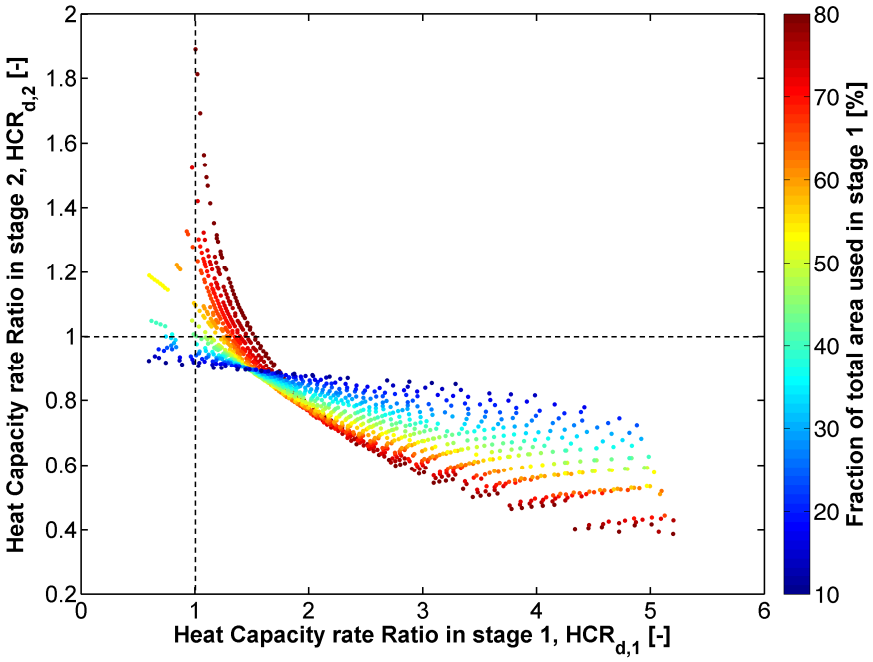

Fig. 12: Variation of $\mathrm{HCR_{d,1}}$ and $\mathrm{HCR_{d,2}}$ with the fraction of total area used in stage 1 (location of extraction/injection).

4.3. The proper direction of extraction

Figure 13 plots the GOR of the various operating points against the amount of air extracted from the humidifier to the dehumidifier. From this graph, it is clear that for the same location of extraction (represented by the color of the points), and for all locations, the GOR of a system with an extraction from the dehumidifier to the humidifier (represented by a negative amount extracted) is always worse than a system without extraction. This means that it is always more advantageous to not extract rather than extract in the wrong direction. A better performance can only be reached by extracting air from the humidifier to the dehumidifier.

This result can be explained by considering the heat capacities of water and saturated air (where $c_p = \frac{\mathrm{d}h}{\mathrm{d}T}|_p$). We first note that the specific heat of water is almost constant in the range of operation of HDH, whereas that of moist air varies greatly with temperature:

$$h_\mathrm{a} = h_\mathrm{da} + \omega_\mathrm{sat} h_\mathrm{v} \tag{21}$$

$$\frac{\mathrm{d}h_\mathrm{a}}{\mathrm{d}T} = c_{p,\mathrm{da}} + \frac{\mathrm{d}\left(\omega_\mathrm{sat} h_\mathrm{v}\right)}{\mathrm{d}T} \tag{22}$$

since the absolute humidity at saturation, ω_sat, varies exponentially with temperature. In order to keep the driving forces constant throughout the exchangers, we need the total heat capacity rates of water and moist

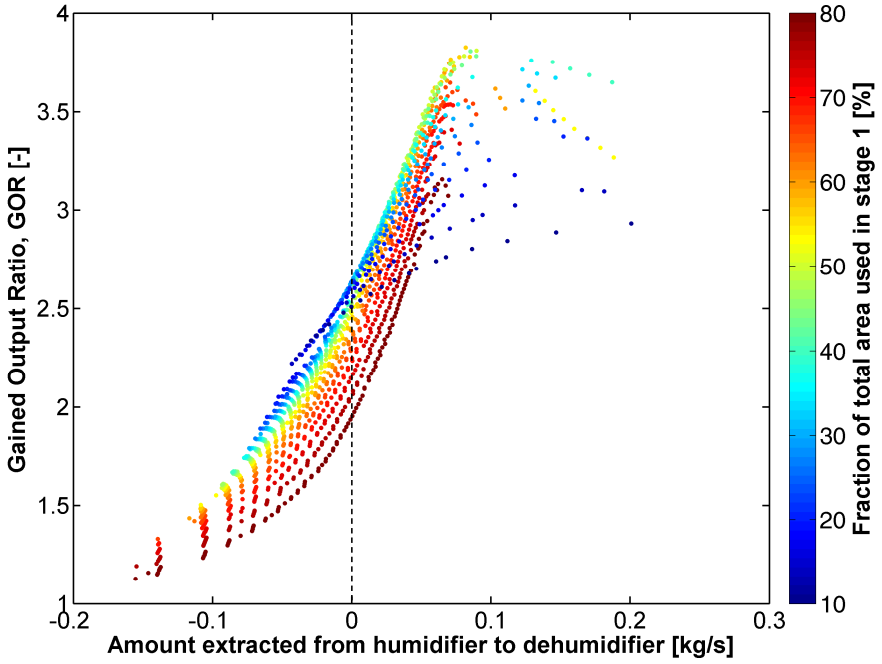

Fig. 13: Variation of GOR with the amount extracted from humidifier to dehumidifier. Note that negative values indicate amount extracted in the other direction.

air to be equal at any location in the exchanger:

$$\left(\dot{m}_{\mathrm{da}}\frac{\mathrm{d}h_{\mathrm{a}}}{\mathrm{d}T}\right)_{\mathrm{loc}} = \left(\dot{m}_{w}\frac{\mathrm{d}h_{\mathrm{w}}}{\mathrm{d}T}\right)_{\mathrm{loc}} \tag{23}$$

$$\mathrm{MR}_{\mathrm{loc}} = \left(\frac{\dot{m}_{\mathrm{w}}}{\dot{m}_{\mathrm{da}}}\right)_{\mathrm{loc}} = \left(\frac{1}{c_{p,\mathrm{w}}}\times\frac{\mathrm{d}h_{\mathrm{a}}}{\mathrm{d}T}\right)_{\mathrm{loc}} \tag{24}$$

where the subscript 'loc' denotes a local variable. Given that $\left(\frac{\mathrm{d}h_{\mathrm{a}}}{\mathrm{d}T}\right)_{\mathrm{loc}}$ increases with temperature whereas the specific heat of water, $c_{p,\mathrm{w}}$, remains constant, the mass flow rate ratio has to increase with temperature in order to reach a better balanced system. This can be done by extracting either air or water from the humidifier to the dehumidifier so that the water-to-air mass flow rate ratio is lower in the colder stages.

Previous attempts to balance HDH systems with the water-heated, closed-air, open-water configuration reported some cases where it was more beneficial to extract air or water from the dehumidifier to the humidifier [25, 26]. This odd finding was possible because the flow rates in the bottom stage were fixed at values that were very far from the optimum, and extracting in the wrong direction could actually make the system perform better. This does not mean that the extraction in that direction is generally correct. It only means that extracting in that direction made the performance better for the specific flow rates that were fixed in the first stage. In fact, for that exact system, a much higher performance can be achieved by choosing the appropriate mass flow rates in both stages instead of fixing a single stage and varying the other stage. The

flow rates in both stages must be treated as variables if overall optimal performance is to be reached. As seen in this paper, the two stages are very interconnected, and the best system performance can only be achieved by simultaneously varying the flow rates in both stages. The approach taken in the previous studies does not reach a global optimum for the two-stage system.

To better visualize this idea, we consider the temperature-enthalpy profiles presented in Fig. 14. Figure 14(a) presents the temperature-enthalpy profile for a system with an air extraction from the dehumidifier to the humidifier, resulting in a GOR of 1.9. If the system was operated at the mass flow rate ratio of the first stage without extraction, the system would achieve a GOR of 1.4. This is one case where extracting from the dehumidifier to the humidifier achieves a better performance, which could lead to the conclusion that it might be beneficial to extract in that direction. However, the same system could achieve a GOR of 2.4 by operating without extraction but with a proper mass flow rate ratio that would result in $\mathrm{HCR_d} = 1$, similar to the profile shown in Fig. 3, and the performance could be improved even further by extracting air from the humidifier to the dehumidifier, resulting in the profile shown in Fig. 14(b), and a GOR of 3.8. Comparing the profiles presented in Fig. 14 leads to the conclusion that it is always desirable to extract from the humidifier to the dehumidifier. The values of the mass flow rate ratio in the two stages that gave the best performance for this system were $\mathrm{MR}_1 = 2.1$ and $\mathrm{MR}_2 = 9.9$. We note that for the case of no extraction the mass flow rate ratio that resulted in a balanced system was $\mathrm{MR} = 4.4$. This proves that in going from a balanced system without extraction to a balanced system with a single extraction we must vary the flow rates in both stages, with the mass flow rate ratio in the first stage being lower than the case of no extraction, and the mass flow rate ratio in the second stage being higher than the case of no extraction.

An interesting conclusion that can be made by considering Fig. 14 is that better performance is achieved when the heat duty is better divided over the available area. In Fig. 14(a), the circles on the temperature profile of the air stream show the intermediate temperatures of the air stream between consecutive dehumidifier trays. At the cold end of the first stage, the spacing between the circles is very small, with some even overlapping, whereas, at the hot end of that stage, the spacing becomes much larger. This indicates that the trays at the cold end of the dehumidifier in the first stage achieve a very small heat duty since they only change the specific enthalpy of air by very small amounts, whereas the trays at the hot end are used to achieve much higher heat and mass transfer rates. This is due to the small driving force in the trays at the cold end. When the system is balanced properly, the trays used achieve comparable rates of heat and mass transfer throughout the system because the driving force is kept relatively constant. This can be seen in Fig. 14(b) with the circles almost equally spaced. Therefore, an easy way to measure experimentally if the system is well balanced is by comparing the heat duty per unit area achieved at different locations in the system.

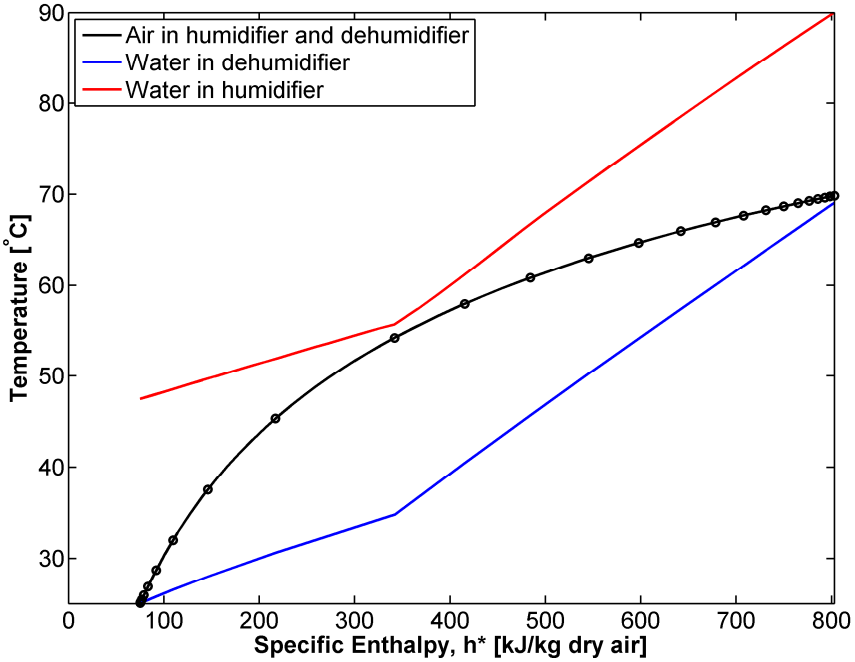

(a) Temperature-enthalpy profile for $MR_1 = 7.9$, $MR_2 = 3.0$. GOR = 1.9, RR = 6.7%.

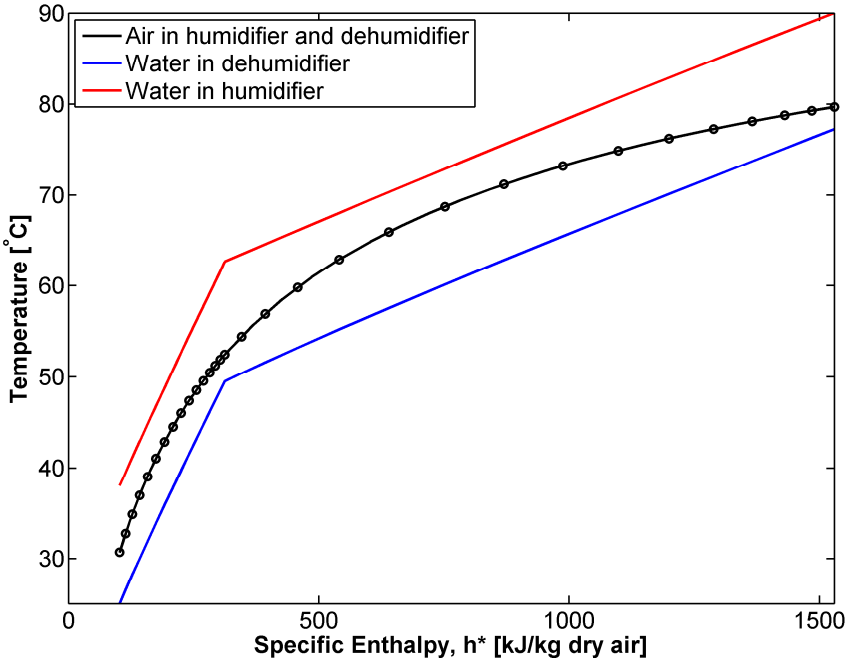

(b) Temperature-enthalpy profile for $MR_1 = 2.1$, $MR_2 = 9.9$. GOR = 3.8, RR = 8.1%.

Fig. 14: Temperature-enthalpy profiles of a system with (a) an extraction from the dehumidifier to the humidifier, and (b) an extraction from the humidifier to the dehumidifier. The dimensions of both systems are summarized in Table 1, and the extraction is such that $N_{t,1} = N_{t,2} = 15$.

5. Conclusions

This paper presents a transport model of a fixed-size HDH system with a single air extraction/injection. The main conclusions drawn from this work are the following:

1. Thermodynamically balancing an HDH system, which is done by setting $\mathrm{HCR_d} = 1$, maximizes energy efficiency and water recovery.
2. Setting $\mathrm{HCR_d} = 1$ minimizes the entropy generation per unit product by minimizing the variances in the driving forces to heat and mass transfer. This results in the best use of the available surface area in the heat and mass exchangers.
3. $\mathrm{HCR_h}$ is not a useful parameter for system performance since it is the ratio of unachievable maxima.
4. A better balanced HDH system can be achieved by extracting air or water from the humidifier to the dehumidifier and setting $\mathrm{HCR_{d,1}} = \mathrm{HCR_{d,2}} = 1$.
5. The extractions in an HDH system should always be from the humidifier to the dehumidifier.
6. The location of the extraction is essential in achieving a balanced system, as not all locations make complete balancing possible.
7. Better system performance is achieved when the heat duty is equally divided over the available area.
8. The effect of thermodynamic balancing is much larger on energy efficiency than on water recovery.

In addition, this paper presents a generalized definition of energy effectiveness of heat and mass exchangers based on the definition by Narayan et al. [36]. The new definition is expressed in Eq. 19 and is rewritten below:

$$\varepsilon = \frac{\Delta \dot{H}}{\Delta \dot{H}_{\mathrm{max}}} = \frac{\Delta \dot{H}}{\Delta \dot{H}|_{\mathrm{pinch}=0}} \tag{19}$$

Acknowledgments

The authors would like to thank the King Fahd University of Petroleum and Minerals for funding the research reported in this paper through the Center for Clean Water and Clean Energy at MIT and KFUPM (Project # R4-CW-08).

References

[1] G. P. Narayan, M. H. Sharqawy, E. K. Summers, J. H. Lienhard V, S. M. Zubair, and M. A. Antar, "The potential of solar-driven humidification-dehumidification desalination for small-scale decentralized water production," *Renewable and Sustainable Energy Reviews*, vol. 14, pp. 1187–1201, 2010.

[2] G. P. Narayan and J. H. Lienhard V, "Humidification-dehumidification desalination," in *Desalination: Water from Water*, Salem, MA: Scrivener Publishing, 2014.

[3] T. Pankratz (Ed.), "HDH tackles brine disposal challenge," *Water Desalination Report*, vol. 50, pp. 2–3, May 2014.

[4] M. Sievers and J. H. Lienhard V, "Design of flat-plate dehumidifiers for humidification-dehumidification desalination systems," *Heat Transfer Engineering*, vol. 34, no. 7, pp. 543–561, 2013.

[5] M. Sievers and J. H. Lienhard V, "Design of plate-fin tube dehumidifiers for humidificationdehumidification desalination systems," *Heat Transfer Engineering*, vol. 36, no. 3, pp. 223–243, 2015.

[6] G. P. Narayan and J. H. Lienhard V, "Thermal design of humidification dehumidification systems for affordable small-scale desalination," *IDA Journal*, vol. 4, no. 3, pp. 24–34, 2012.

[7] G. P. Narayan, M. H. Sharqawy, S. Lam, S. K. Das, and J. H. Lienhard V, "Bubble columns for condensation at high concentrations of noncondensable gas: Heat-transfer model and experiments," *AIChE Journal*, vol. 59, no. 5, pp. 1780–1790, 2013.

[8] E. W. Tow and J. H. Lienhard V, "Experiments and modeling of bubble column dehumidifier performance," *International Journal of Thermal Sciences*, vol. 80, pp. 65 – 75, 2014.

[9] E. W. Tow and J. H. Lienhard V, "Analytical modeling of a bubble column dehumidifier," in *Proceedings of the ASME 2013 Summer Heat Transfer Conference*, no. HT2013-17763, Minneapolis, MN, July 2013.

[10] E. W. Tow and J. H. Lienhard V, "Heat flux and effectiveness in bubble column dehumidifiers for HDH desalination," in *IDA World Congress on Desalination and Water Reuse*, Tianjin, China, October 2013.

[11] E. W. Tow and J. H. Lienhard V, "Heat transfer to a horizontal cylinder in a shallow bubble column," *International Journal of Heat and Mass Transfer*, vol. 79, pp. 353 – 361, 2014.

[12] E. W. Tow and J. H. Lienhard V, "Measurements of heat transfer coefficients to cylinders in shallow bubble columns," in *Proc. 15th Intl. Heat Transfer Conference, IHTC-15*, no. IHTC15-8857, Kyoto, Japan, August 2014.

[13] K. M. Chehayeb, F. K. Cheaib, and J. H. Lienhard V, "A numerical solution algorithm for a heat and mass transfer model of a desalination systems based on packed-bed humidification and bubble column dehumidification," in *Proc. 15th Intl. Heat Transfer Conference, IHTC-15*, no. IHTC15-8995, Kyoto, Japan, August 2014.

[14] K. H. Mistry, J. H. Lienhard V, and S. M. Zubair, "Effect of entropy generation on the performance of humidification-dehumidification desalination cycles," *International Journal of Thermal Sciences*, vol. 49, pp. 1837–47, 2010.

[15] K. H. Mistry, R. K. McGovern, G. P. Thiel, E. K. Summers, S. M. Zubair, and J. H. Lienhard V, "Entropy generation analysis of desalination technologies," *Entropy*, vol. 13, p. 182964, 2011.

[16] H. Müller-Holst, *Solar thermal desalination using the Multiple Effect Humidification (MEH) method in Solar Desalination for the 21st Century*, ch. 15, pp. 215–25. NATO Security through Science Series, Springer, Dordrecht, 2007.

[17] H. Müller-Holst, *Mehrfacheffekt-Feuchtluftdestillation bei Umgebungsdruck - Verfahrensoptimierung und Anwendungen*. PhD thesis, Technische Universität Berlin, 2002.

[18] M. Zamen, S. M. Soufari, and M. Amidpour, "Improvement of solar humdification-dehumidification desalination using multi-stage process," *Chemical Engineering Transactions*, vol. 25, pp. 1091–1096, 2011.

[19] R. K. McGovern, G. P. Thiel, G. P. Narayan, S. M. Zubair, and J. H. Lienhard V, "Performance limits of zero and single extraction humidification-dehumidification desalination systems," *Applied Energy*, vol. 102, pp. 1081 – 1090, 2013.

[20] G. P. Thiel and J. H. Lienhard V, "Entropy generation in condensation in the presence of high concentrations of noncondensable gases," *International Journal of Heat and Mass Transfer*, vol. 55, pp. 5133–5147, May 2012.

[21] G. P. Narayan, J. H. Lienhard V, and S. M. Zubair, "Entropy generation minimization of combined heat and mass transfer devices," *International Journal of Thermal Sciences*, vol. 49, pp. 2057–66, 2010.

[22] G. P. Narayan, K. M. Chehayeb, R. K. McGovern, G. P. Thiel, S. M. Zubair, and J. H. Lienhard V, "Thermodynamic balancing of the humidification dehumidification desalination system by mass extraction and injection," *International Journal of Heat and Mass Transfer*, vol. 57, pp. 756 – 770, 2013.

[23] K. M. Chehayeb, G. Prakash Narayan, S. M. Zubair, and J. H. Lienhard V, "Use of multiple extractions and injections to thermodynamically balance the humidification dehumidification desalination system," *International Journal of Heat and Mass Transfer*, vol. 68, pp. 422–434, 2014.

[24] G. P. Narayan, M. G. St. John, S. M. Zubair, and J. H. Lienhard V, "Thermal design of the humidification dehumidification desalination system: An experimental investigation," *International Journal of Heat and Mass Transfer*, vol. 58, pp. 740 – 748, 2013.

[25] J. A. Miller and J. H. Lienhard V, "Impact of extraction on a humidification dehumidification desalination system," *Desalination*, vol. 313, pp. 87 – 96, 2013.

[26] G. P. Thiel, J. A. Miller, S. M. Zubair, and J. H. Lienhard V, "Effect of mass extractions and injections on the performance of a fixed-size humidification dehumidification desalination system," *Desalination*, vol. 314, pp. 50 – 58, 2013.

[27] K. M. Chehayeb, "Numerical fixed-effectiveness and fixed-area models of the humidification dehumidification desalination system with air extractions and injections," Master's thesis, Massachusetts Institute of Technology, Cambridge, MA, 2014.

[28] J. C. Kloppers, *A critical evaluation and refinement of the performance prediction of wet-cooling towers*. PhD thesis, Stellenbosch: University of Stellenbosch, 2003.

[29] W. D. Deckwer, "On the mechanism of heat transfer in bubble column reactors," *Chemical Engineering Science*, vol. 35, no. 6, pp. 1341–1346, 1980.

[30] Y. Mori and W. Nakayama, "Study on forced convective heat transfer in curved pipes: (1st report, laminar region)," *International Journal of Heat and Mass Transfer*, vol. 8, no. 1, pp. 67 – 82, 1965.

[31] Y. Mori and W. Nakayama, "Study of forced convective heat transfer in curved pipes (2nd report, turbulent region)," *International Journal of Heat and Mass Transfer*, vol. 10, no. 1, pp. 37–59, 1967.

[32] M. Poppe and H. Rögener, "Berechnung von rückkühlwerken," *VDI-Wärmeatlas*, vol. 111, pp. 1–15, 1991.

[33] J. Kloppers and D. Kröger, "A critical investigation into the heat and mass transfer analysis of counterflow wet-cooling towers," *International Journal of Heat and Mass Transfer*, vol. 48, pp. 765–777, 2005.

[34] K. H. Mistry, A. Mitsos, and J. H. Lienhard V, "Optimal operating conditions and configurations for humidification-dehumidification desalination cycles," *International Journal of Thermal Sciences*, vol. 50, pp. 779–789, 2011.

[35] G. P. Thiel, R. K. McGovern, S. M. Zubair, and J. H. Lienhard V, "Thermodynamic equipartition for increased second law efficiency," *Applied Energy*, vol. 118, pp. 292 – 299, 2014.

[36] G. P. Narayan, K. H. Mistry, M. H. Sharqawy, S. M. Zubair, and J. H. Lienhard V, "Energy effectiveness of simultaneous heat and mass exchange devices," *Frontiers in Heat and Mass Transfer*, vol. 1, no. 2, pp. 1–13, 2010.

[37] F. Bosnjaković, *Technical thermodynamics*. Holt, Rinehart and Winston, 1965.

[38] M. H. Sharqawy, J. H. Lienhard V, and S. M. Zubair, "Thermophysical properties of seawater: A review of existing correlations and data," *Desalination and Water Treatment*, vol. 16, pp. 354–80, 2010.

[39] S. Herrmann, H.-J. Kretzschmar, and D. P. Gatley, "Thermodynamic properties of real moist air, dry air, steam, water, and ice (rp-1485)," *HVAC&R Research*, vol. 15, no. 5, pp. 961–986, 2009.

Appendix A. Correlations used in modeling the bubble column dehumidifier

The following are the correlations used to model the resistances in the bubble column dehumidifier model: For the outer resistance, $R_{\text{out}} = \frac{1}{h_t A_{out}}$, we used the correlation by Deckwer [29] in dimensional form, where h_t is the heat transfer coefficient:

$$h_t = 0.1 k_f^{1/2} \rho_f^{3/4} c_{p,f}^{1/2} \mu_f^{-1/4} g^{1/4} V_g^{1/4} \tag{A.1}$$

For the inner resistance, R_{in}, we used the correlations by Mori and Nakayama [30, 31].
In the laminar regime:

$$Nu_D = \frac{h_t D_{in}}{k} = 0.8636 \frac{K^{1/2}}{Z} \tag{A.2}$$

$$K = Re \left(\frac{D_{in}}{D_{coil}} \right)^{1/2} \tag{A.3}$$

$$Z = \frac{2}{11} \left(1 + \sqrt{1 + \frac{77}{4} Pr^{-2}} \right) \tag{A.4}$$

In the turbulent regime:

$$Nu_D = \frac{h_t D_{in}}{k} = \frac{1}{41} Pr^{0.4} Re^{5/6} \left(\frac{D_{in}}{D_{coil}} \right)^{1/12} \{1 + \frac{0.061}{\left[Re \left(\frac{D_{in}}{D_{coil}} \right)^{2.5} \right]^{1/6}} \} \tag{A.5}$$

Appendix B. Equations used in modeling the packed-bed humidifier

The equations below are taken from the work by Kloppers and Kröger [33], and describe the Poppe and Rögener model [32]. The solution procedure was also taken from Kloppers and Kröger [33], and greater detail can be found in Klopper's doctoral thesis [28].

Appendix B.1. Unsaturated air

The Lewis factor according to Bosnjakovic [37]:

$$Le_f = 0.865^{0.667} \left(\frac{\omega_{sw} + 0.622}{\omega + 0.622} - 1 \right) \left[\ln \left(\frac{\omega_{sw} + 0.622}{\omega + 0.622} \right) \right]^{-1} \tag{B.1}$$

The variation of h_a with T_w:

$$\begin{aligned} \frac{dh_a}{dT_w} &= \frac{\dot{m}_w c_{p,w}}{\dot{m}_a} \\ &\times \left(1 + \frac{(\omega_{sw} - \omega) c_{p,w} T_w}{h_{a,sw} - h_a + (Le_f - 1)[h_{a,sw} - h_a - (\omega_{sw} - \omega) h_v] - (\omega_{sw} - \omega) c_{p,w} T_w} \right) \end{aligned} \tag{B.2}$$

The variation of ω with T_w:

$$\begin{aligned} \frac{d\omega}{dT_w} &= \frac{\dot{m}_w c_{p,w}}{\dot{m}_a} \\ &\times \frac{\omega_{sw} - \omega}{h_{a,sw} - h_a + (Le_f - 1)[h_{a,sw} - h_a - (\omega_{sw} - \omega) h_v] - (\omega_{sw} - \omega) c_{p,w} T_w} \end{aligned} \tag{B.3}$$

The variation of Me with T_{w}:

$$\frac{\mathrm{d}Me}{\mathrm{d}T_{\mathrm{w}}} = \frac{c_{p,\mathrm{w}}}{h_{\mathrm{a,sw}} - h_{\mathrm{a}} + (Le_{\mathrm{f}} - 1)\left[h_{\mathrm{a,sw}} - h_{\mathrm{a}} - (\omega_{\mathrm{sw}} - \omega)\, h_{\mathrm{v}}\right] - (\omega_{\mathrm{sw}} - \omega)\, c_{p,\mathrm{w}} T_{\mathrm{w}}} \tag{B.4}$$

The subscript 'sw' means that the property is evaluated at saturation at the water temperature.

Appendix B.2. Supersaturated air

Lewis factor according to Bosnjakovic [37]

$$Le_{\mathrm{f}} = 0.865^{0.667} \left(\frac{\omega_{\mathrm{sw}} + 0.622}{\omega_{\mathrm{sa}} + 0.622} - 1\right) \left[\ln\left(\frac{\omega_{\mathrm{sw}} + 0.622}{\omega_{\mathrm{sa}} + 0.622}\right)\right]^{-1} \tag{B.5}$$

$$\begin{aligned} X = {} & h_{\mathrm{a,sw}} - h_{\mathrm{a,ss}} + (Le_{\mathrm{f}} - 1)\left[h_{\mathrm{a,sw}} - h_{\mathrm{a,ss}} - (\omega_{\mathrm{sw}} - \omega_{\mathrm{sa}})\, h_{\mathrm{v}} - (\omega_{\mathrm{sa}} - \omega)\, c_{p,\mathrm{w}} T_{\mathrm{w}}\right] \\ & - (\omega_{\mathrm{sw}} - \omega)\, c_{p,\mathrm{w}} T_{\mathrm{w}} \end{aligned} \tag{B.6}$$

$$\frac{\mathrm{d}h_{\mathrm{a}}}{\mathrm{d}T_{\mathrm{w}}} = \frac{\dot{m}_{\mathrm{w}} c_{p,\mathrm{w}}}{\dot{m}_{\mathrm{a}}} \left(1 + \frac{(\omega_{\mathrm{sw}} - \omega_{\mathrm{sa}})\, c_{p,\mathrm{w}} T_{\mathrm{w}}}{X}\right) \tag{B.7}$$

$$\frac{\mathrm{d}\omega}{\mathrm{d}T_{\mathrm{w}}} = \frac{\dot{m}_{\mathrm{w}} c_{p,\mathrm{w}}}{\dot{m}_{\mathrm{a}}} \left(\frac{\omega_{\mathrm{sw}} - \omega_{\mathrm{sa}}}{X}\right) \tag{B.8}$$

$$\frac{\mathrm{d}Me}{\mathrm{d}T_{\mathrm{w}}} = \frac{c_{p,\mathrm{w}}}{X} \tag{B.9}$$

The subscript 'sa' means that the property is evaluated at saturation at the air temperature, and the subscript 'ss' denotes supersaturation.

Appendix C. Thermophysical properties

The thermophysical properties of seawater were evaluated using the correlations presented by Sharqawy et al. [38]. In addition to its effect on the properties of water, we also have to look at the effect of salinity on the vapor pressure in the humidifier as the air is in direct contact with saline water. We use Raoult's law to relate the vapor pressure of seawater to that of pure water [38]:

$$\frac{P_{\mathrm{v,pw}}}{P_{\mathrm{v,w}}} = 1 + 0.57357 \times \frac{S}{1000 - S} \tag{C.1}$$

The thermophysical properties of moist air and water vapor were evaluated using the ASHRAE Library of Humid Air Psychrometric & Transport Property (LibHuAirProp) which is based on ASHRAE RP-1485 [39].

Appendix D. Solution algorithm for a system with a single air extraction

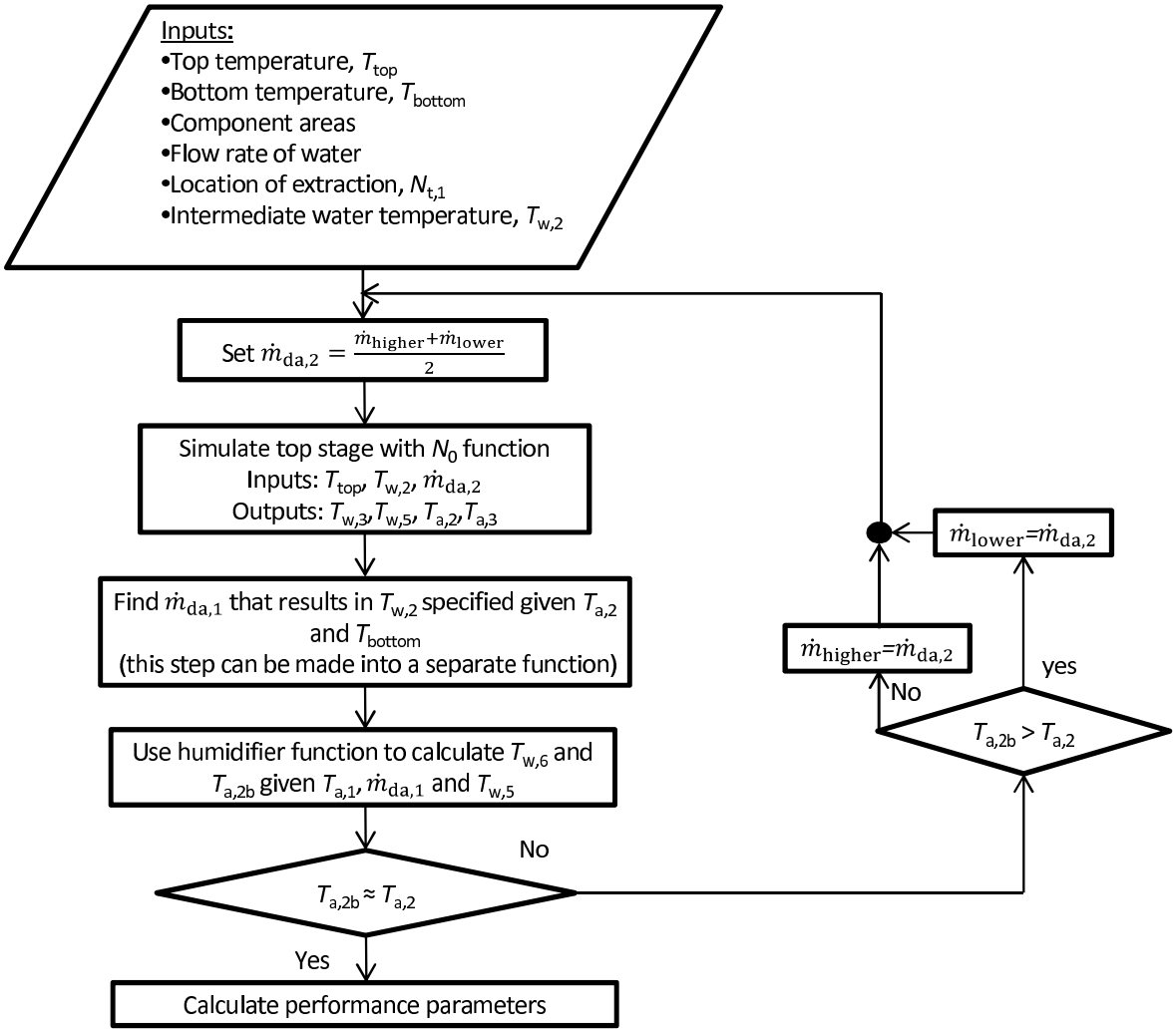

Fig. D.15: Solution algorithm for the complete HDH system with a single extraction.

List of Figures

Contents